NUMERICAL ANALYSIS OF NANOFLUID FLOW IN A CONICAL HELICAL TUBE

Majdi Ahmed Misbah ALI

2022
MASTER THESIS
MECHANICAL ENGINEERING DEPARTMENT

Thesis Advisor
Prof. Dr. Kamil ARSLAN

NUMERICAL ANALYSIS OF NANOFLUID FLOW IN A CONICAL HELICAL TUBE

Majdi Ahmed Misbah ALI

T.C.
Karabuk University
Institute of Graduate Programs
Department of Mechanical Engineering
Prepared As
Master Thesis

Thesis Advisor
Prof. Dr. Kamil ARSLAN

KARABUK
April 2022

I certify that in my opinion the thesis submitted by Majdi Ahmed Misbah ALI titled "NANOFLUID FLOW AND HEAT TRANSFER ANALYSIS IN A CONICAL HELICAL" is fully adequate in scope and quality as a thesis for the degree of Master of Science.

Prof. Dr. Kamil ARSLAN .....
Thesis Advisor, Department of Mechanical Engineering

This thesis is accepted by the examining committee with a unanimous vote in the Department of Mechanical Engineering as a Master of Science thesis. 22/4/2022

Examining Committee Members (Institutions)	Signature
Chairman : Asst. Prof. Dr. Hüseyin KAYA (BÜ)	.....
Member : Prof. Dr. Kamil ARSLAN (KBÜ)	.....
Member : Assoc. Prof. Dr. Engin GEDİK (KBÜ)	.....

The degree of Master of Science by the thesis submitted is approved by the Administrative Board of the Institute of Graduate Programs, Karabuk University.

Prof. Dr. Hasan SOLMAZ .....
Director of the Institute of Graduate Programs

"I declare that all the information within this thesis has been gathered and presented in accordance with academic regulations and ethical principles and I have according to the requirements of these regulations and principles cited all those which do not originate in this work as well."

Majdi Ahmed Misbah AlI

ABSTRACT

M. Sc. Thesis

NUMERICAL ANALYSIS OF NANOFLUID FLOW IN A CONICAL HELICAL TUBE

Majdi Ahmed Misbah ALI

Karabuk University
Institute of Graduate Programs
The Department of Mechanical Engineering

Thesis Advisor:
Prof. Dr. Kamil ARSLAN
April 2022, 74 pages

In this study, nanofluid flow in conical helical tube has been numerically investigated. The study has been carried out in three-dimensional laminar flow ($1050 \leq Re \leq 2150$) conditions. Conical helical tube with 170 mm base diameter, 10 mm tube diameter and 1500 mm length has been used in the study. Constant heat flux of 1000 W/m^2 has been implemented on the tube surface. Al_2O_3 – water nanofluid with different nanoparticle volume fractions ratio (1.0%, 2.0%, and 3.0%) has also been used as the working fluid in the numerical analyzes. In addition, studies have been carried out for blade, platelet and cylindrical nanoparticle shapes.

The average Nusselt numbers and the average Darcy friction factors have been used to estimate the flow and heat transfer characteristics of nanofluid flow in the conical helical tubes with different nanoparticle volume fractions and shapes. Pressure and temperature distribution inside the conical helical tubes have been also examined for different cases. Secondary flows in conical helical tubes have been analyzed in

detail. Numerical results of the study have been also presented as the variation of average Nusselt number and Darcy friction factor with Reynolds number, nanoparticle shape and nanoparticle volume fraction. As a result, the highest convective heat transfer performance has been obtained for platelet nanoparticle shape of the 3.0% Al_2O_3-water nanofluid.

Keywords **:** Conical helical tubes, Ansys, nanofluid, CFD, convective heat transfer.

Science Code : 91412

ÖZET

Yüksek Lisans Tezi

KONİK HELİSEL BİR TÜP İÇERİSİNDEKİ NANOAKIŞKAN AKIŞI VE ISI TRANSFERİ ANALİZİ

Majdi Ahmed Misbah ALI

Karabük Üniversitesi
Lisansüstü Eğitim Enstitüsü
Makine Mühendisliği Anabilim Dalı

Tez Danışmanı:
Prof. Dr. Kamil ARSLAN
Nisan 2022, 74 sayfa

Bu çalışmada, konik sarmal tüplerdeki nanoakışkan akışı sayısal olarak incelenmiştir. Çalışma, üç boyutlu laminer akış ($1050 \leq Re \leq 2150$) koşullarında gerçekleştirilmiştir. Çalışmada 170 mm taban çapına, 10 mm boru çapına ve 1500 mm uzunluğa sahip konik sarmal boru kullanılmıştır. Al_2O_3 – su nanoakışkanı farklı nanoparçacık hacim oranlarında (%1.0, %2.0, %3.0) çalışma akışkanı olarak kullanılmıştır. Ayrıca kullanılan nanoparçacıklar bıçak, plaket ve silindirik olmak üzere üç farklı şekilde kullanılarak çalışmalar yapılmıştır.

Konik sarmal borulardaki akış ve ısı transfer performansını tahmin etmek için ortalama Nusselt sayıları ve ortalama Darcy sürtünme faktörleri hesaplanmıştır. Çalışmanın sonuçları her bir nanoparçacık şekli için %1.0, %2.0, %3.0 nanoparçacık hacim oranları için elde edilmiştir. Konik sarmal boruların içindeki basınç ve sıcaklık dağılımı da farklı durumlar için incelenmiştir. Konik sarmal borulardaki ikincil

akışlar ayrıntılı olarak analiz edilmiştir. Çalışmanın sayısal sonuçları ortalama Nusselt sayısı ve Darcy sürtünme faktörünün Reynolds sayısı ile değişimi ve her bir nanoparçacık şekli ve nanoparçacık hacim oranı için ayrı olarak sunulmuştur. Sonuç olarak, en yüksek taşınımla ısı transfer performansı %3.0 Al_2O_3-su nanoakışkanın plaket nanoparçacık şekli için elde edilmiştir.

Anahtar Kelimeler: Konik helisel tüpler, ANSYS, nanoakışkan, HAD, taşınım ile ısı transferi.

Bilim Kodu **:** 91412

ACKNOWLEDGMENT

Firstly, I would like to expand the scope of my thanks and appreciation to Prof. Dr. Kamil ARSLAN, a member of the faculty at the Department of Mechanical Engineering in Karabük University, who provided his entire interest and support for this thesis from planning to implementation, her knowledge, and experiences, and put this study on a scientific basis with his guidance and assistance to complete the research requirements. I am very grateful to the faculty members of the Mechanical Engineering department, who invested the energy to provide guidance to me. I also want to thank my family and all my close friends. Finally, this thesis is dedicated to my mom and my all brothers.

CONTENTS

Page

APPROVAL ii
ABSTRACT iv
ÖZET vi
ACKNOWLEDGMENT viii
CONTENTS ix
LIST OF FIGURES xi
LIST OF TABLES xiii
SYMBOLS AND ABBREVIATIONS xiv

PART 1 1
INTRODUCTION 1
1.1. THERMAL MANAGEMENT SYSTEMS 1
1.2. NANOFLUIDS 3
1.2.1. Mechanism of Heat transfer in Nanofluids 3
1.2.2. Important Characteristics of Nanoparticles 5
1.2.3. Thermophysical Properties of Nanofluids 7
1.2.3.1. Thermal Conductivity 7
1.2.3.2. Specific Heat 11
1.2.3.3. Density 12
1.2.3.4. Viscosity 12
1.2.4. Potential Applications of Nanofluids 14
1.3. HEAT EXCHANGER AND HEAT SINKS 14
1.4. PROBLEM STATEMENT 17
1.5. OBJECTIVES OF STUDY 17
1.6. SCOPE OF STUDY 18

PART2 19
LITERATURE REVIEW 19
2.1. HEAT EXCHANGER 19

Page

2.2. POTENTIAL OF NANOFLUIDS FOR HEAT EXCHANGERS 21
2.2.1. Nanofluids Performance in Flattened Tube Heat Exchangers 21
2.2.2. Nanofluid Performance in Helical Tube Heat Exchangers 25
PART 3 43
MATERIAL AND METHOD 43
3.1. IMPORTANT DEFINITIONS 43
3.2. CALCULATE THE TERMOPHYSICAL PROPERTIES OF NANOFLUIDS 44
3.3. NUMERICAL SIMULATION 47
3.3.1. Creating Geometry 49
3.3.2. Creating Mesh 49
3.3.3. Defining the Problem and Boundary Conditions 50
3.3.4. Analysis 51
3.3.5. Analyze the Results 51

PART 4 52
RESULTS AND DISCUSSIONS 52
4.1. MESH OPTIMIZATION AND VALIDATION OF THE NUMERICAL CODE 52
4.2. EFFECT OF CHANGING NANOPARTICLE ON AVERAGE NUSSELT NUMBER 54
4.3.1. Effect the Nanoparticles Volume Ratio on Average Nusselt Number 54
4.2.2. Effect of Nanoparticle Shape on Average Nusselt Number 56
4.5. PERFORMANCE EVALUATION CRITERIA 60

PART 5 63
CONCLUSION AND RECOMMENDATIONS 63
5.1. CONCLUSION 63
5.2. RECOMMENDATIONS 64

REFERENCES 65

CURRICULUM VITAE ..... **Hata! Yer işareti tanımlanmamış.**

LIST OF FIGURES

Page

Figure 1.1. Nanoparticles used in nanofluids' preparation 3

Figure 1.2. Nanofluid preparation method (a) single step method and (b) two-step method 4

Figure 1.3. Preparation of nanofluid in bulk quantity through two-step nanofluid preparation method (a) nanofluid preparation steps, (b) ferric oxide nanoparticles, (c) titanium dioxide nanoparticles, and (d) produced nanofluid in container 5

Figure 1.4. Nanofluid characteristics 7

Figure 1.5. Influence of particle concentration on thermal conductivity of nanofluid 8

Figure 1.6. Effect of base fluid on thermal conductivity of the nanofluid 9

Figure 1.7. Influence of nanoparticle size on thermal conductivity of nanofluid 9

Figure 1.8. Effect of temperature on thermal conductivity o nanofluid. 10

Figure 1.9. Nanoparticle shape effect on thermal conductivity of nanofluid 11

Figure 1.10. CAD model of flat tube heat exchanger 16

Figure 1.11. Example of heat sink experimental setup 16

Figure 2.1. Selection criterion of heat exchanger tubes 20

Figure 2.2. Geometries of heat exchangers, (a) Helical tube, (b) Flat tube, (c) Conical tube, (d) Spiral tube with varying curvature and (d) Spiral tube 21

Figure 2.3. Nanofluids test setup for flat tube radiator heat exchanger (a) Experimental setup and (b) Schematic diagram 22

Figure 2.4. Repeatability tests for heat transfer rate after 3 days of initial testing .. 22

Figure 2.5. Geometry design of double pipe helical tube (a) Single section and (b) Full tube 26

Figure 2.6. Test section arrangement for helical tube heat exchanger using nanofluid (a) Schematic representation and (b) Experimentation setup 27

Figure 2.7. Computational domain 29

Figure 2.8. Schematic of helical tubes and conical helical tube 29

Figure 2.9. Illustration of the experimental platform and how it works 30

Figure 2.10. Technical appearance of the model 31

Page

Figure 2.11. The effect of the change of nanoparticle shapes on the average Nusselt number of nanofluid with 1.0%, 2.0% and 3.0% nanoparticle volumetric ratio 32

Figure 3.1. General view of commonly used nanoparticle types 45

Figure 3.2. Schematic diagram of conical coil tube. 49

Figure 3.4. Thermophysical properties of the working fluid. 51

Figure 3.5. Residuals monitors. 51

Figure 4.2. Effect of the platelet nanoparticle volume ratio on average Nusselt number. 54

Figure 4.3. Effect of the blade shape nanoparticle volume ratio on average Nusselt number. 55

Figure 4.4. Effect of the cylindrical shape nanoparticle volume ratio on average Nusselt number. 55

Figure 4.5. Effect of the nanoparticle shape at 1.0% nanoparticle volume ratio on the average Nusselt number. 56

Figure 4.6. Effect of the nanoparticle shape at 2.0% nanoparticle volume ratio on the average Nusselt number. 57

Figure 4.7. Effect of the change of nanoparticle shape at 3.0% nanoparticle volume ratio on the average Nusselt number. 57

Figure 4.8. Temperature distribution of 3.0% nanoparticle volume ratio of Al_2O_3-water nanofluid with platelet nanoparticle in the tube. 58

Figure 4.9. Temperature distribution of 3.0% nanoparticle volume ratio of Al_2O_3-water nanofluid with platelet nanoparticle at the outlet section. 58

Figure 4.10. Effect of the nanoparticle shape at 1.0% nanoparticle volume ratio on the average Darcy friction factor. 59

Figure 4.11. Effect of the nanoparticle shape at 2.0% nanoparticle volume ratio on the average Darcy friction factor. 59

Figure 4.12. Effect of the nanoparticle shape at 3.0% nanoparticle volume ratio on the average Darcy friction factor. 60

Figure 4.13. Variation of *PEC* value according to nanoparticle type at 1.0% nanoparticle volume ratio. 60

Figure 4.14. Variation of *PEC* value according to nanoparticle type at 2.0% nanoparticle volume ratio. 61

Figure 4.15. Variation of *PEC* value according to nanoparticle type at 3.0% nanoparticle volume ratio. 61

Figure 4.16. Pressure distribution on in the tube. 62

LIST OF TABLES

Page

Table 2.1. Computational grids. 28

Table 2.2. Major findings of some of the recent studies on nanofluids in heat exchangers. 33

Table 3.1. Thermophysical properties of nanoparticle and base fluid 45

Table 3.2. Surface resistance and shape effects of Al_2O_3 nanoparticle 46

Table 3.3. Viscosity coefficient for different nanoparticle shapes..... 46

Table 3.4. Coiled conical tube dimensions. 49

Table 4.1. Variation of *Nu* and *f* with mesh number. 52

Table 4.2. Comparison of the results of numerical analysis with literature (pure water). 53

SYMBOLS AND ABBREVIATIONS

SYMBOLS

Nu	: Nusselt number
Re	: Reynolds number
f	: Friction factor
C_p	: Heat capacity
q"	: Heat flux
k	: Heat conductivity
b	: Heat Bulk
d	: Diameter of tube
T	: Temperature
T_i	: Temperature inlet
T_o	: Temperature outlet
P	: Pressure
V	: Velocity of fluid
μ	: Viscosity of fluid
ρ	: Density of fluid
P_i	: Pressure inlet
P_o	: Presser outlet
ΔP	: Pressure difference
h	: Convective Heat Transfer
Φ	: Nanoparticle volume

ABBREVIATIONS

PEC	: Performance Evaluation Criteria
CHTC	: Convective heat transfer coefficient
NF	: Nanofluid

NP : Nanoparticle

CFD : Computational fluid dynamics

PART 1

INTRODUCTION

1.1. THERMAL MANAGEMENT SYSTEMS

Passive methods of thermal management mainly utilize the natural flow of air to minimalize the temperature of the mechanical and the electronic components. Passive method of thermal management mainly focuses on the geometry of the heat exchangers and the material of cooling/thermal management of electronic and mechanical devices is major challenge in variety of applications. Thermal management of a system is mainly dependent on the type of coolant/working fluid and the geometry and the material of the heat exchangers. A range of conventional and modern thermal fluids and heat exchanger channel geometries have been proposed and tested for potential use in thermal management applications [1,2].

- Active-Method of Thermal Management.
- Passive-Method of Thermal Management.

Passive methods of thermal management mainly utilize the natural flow of air to minimalize the temperature of the mechanical and the electronic components. Passive method of thermal management mainly focuses on the geometry of the heat exchangers and the material of cooling/thermal management of electronic and mechanical devices is major challenge in variety of applications. Thermal management of a system is mainly dependent on the type of coolant/working fluid and the geometry and the material of the heat exchangers. A range of conventional and modern thermal fluids and heat exchanger channel geometries have been proposed and tested for potential use in thermal management applications [1,2].

Due to complexity of geometrical designs and manufacturing complications, the cost of thermal management systems gets increased. To overcome the challenges and improve the rate of thermal transportation through the heat exchangers, active methods of cooling were employed that mainly make use of forced convection heat transfer mechanism. Most of the modern thermal management systems make use of forced convection heat transfer mechanism to perform the cooling operation of components [3]. Some of the critical factors that influence the effectiveness of convection heat transfer in thermal management systems are listed as follows:

- Thermal characteristics of the coolant
- Rheological characteristics of the coolant
- Surface properties of the flow channel
- Heat transfer surface area
- Heat sink geometry

Conventional cooling methods used water and air as the coolant in thermal management devices. However, thermal transportation and flow characteristics of these conventional fluids do not meet the requirements of modern thermal management devices. Therefore, significant improvement has been brought to the geometry of heat exchanging sections as well as modern thermal fluids have been developed to counteract the challenge of overheating in the electronic and mechanical devices [4]. Some of the conventional coolants are given below.

- Air
- Water
- Ethylene glycol
- Thermal oil.

Scientists of different laboratories have been working for years to develop some efficient thermal fluids. One of the modern thermal fluids that possess impressive thermal transportation characteristics is called nanofluid. Nanofluids are one of the newly developed thermo-fields that possess superior thermal and fluidic characteristics as compared to the conventional fluids [5].

1.2. NANOFLUIDS

1.2.1. Mechanism of Heat transfer in Nanofluids

Nanofluids possess superior thermal characteristics as compared to conventional thermal fluids. There are various types of nanofluids that include:

- Mono nanofluids
- Hybrid nanofluids
- Ionic nanofluids.

Superior thermal characteristics of nanofluids are mainly due to improved thermal conductivity of the base fluid and the available surface are due to the colloidal suspension of metallic particles. Nanoparticles' properties play significant role in overall success of the nanofluids. Types of nanoparticles used in the making of nanofluids have been presented in the (Fig 1.1) [6].

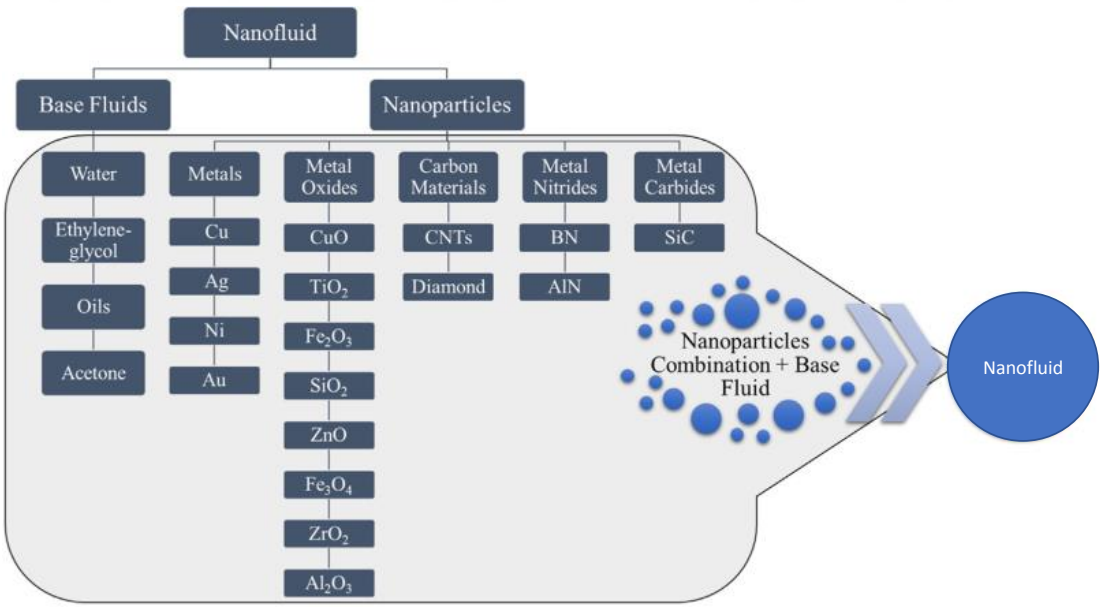

Figure 1.1. Nanoparticles used in nanofluids' preparation [6].

Preparation of nanofluids is carried out by two different methods.

- Single-step method of nanofluid preparation
- Two-step method of nanofluid preparation.

Both abovementioned methods of nanofluid preparation have been explained in (Fig 1.2) [7]. Single-step method involves simultaneous production of preparation through hot wire method and nanofluid production. Whereas, in two-step method, nanoparticles are produced through various mechanical methods of nano-powder production and then the fluid is produced through suspension creation methods. Single-step method results is more stable suspension; however, this method of nanofluid production is quite expensive as compared to the two-step method. Single-step method is preferred for small production purposes however, for industrial or bulk production of nanofluids, two step method is used (Fig 1.3) [7].

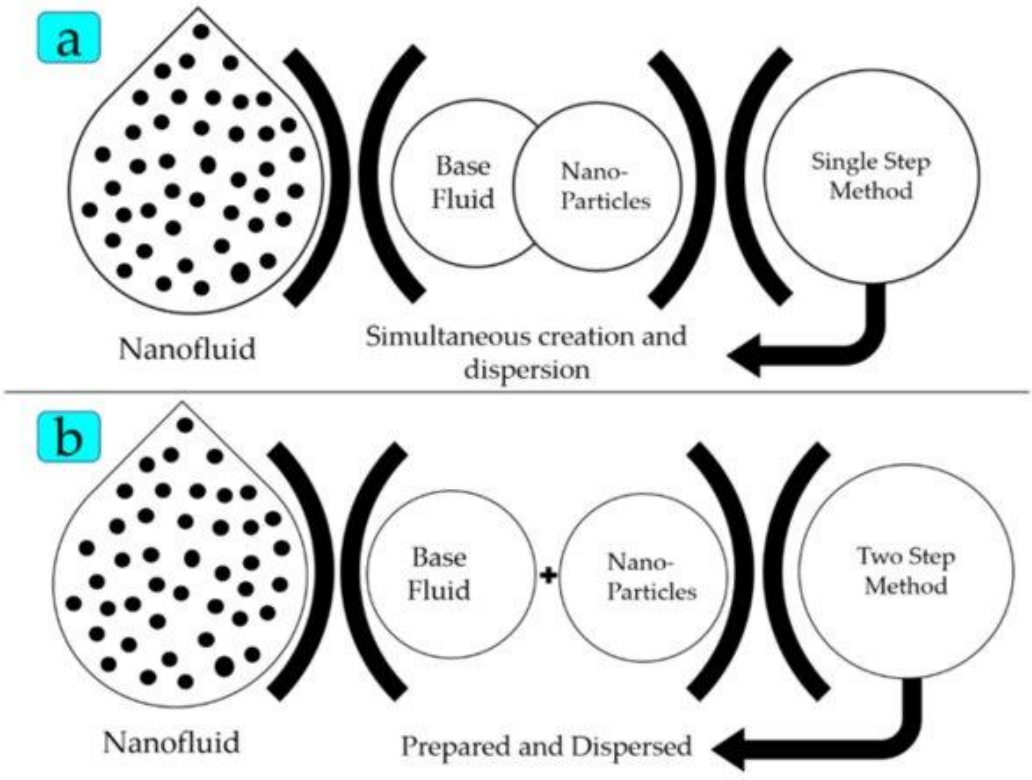

Figure 1.2. Nanofluid preparation method (a) Single step method and (b) Two-step method [7].

Figure 1.3. Preparation of nanofluid in bulk quantity through two-step nanofluid preparation method (a) nanofluid preparation steps, (b) ferric oxide nanoparticles, (c) titanium dioxide nanoparticles, and (d) produced nanofluid in container [7].

1.2.2. Important Characteristics of Nanoparticles

- Size of the nanoparticles
- Shape of the nanoparticles
- Thermal conductivity of nanofluid
- Intermolecular attraction/clustering effect.

Size and shape of the nanoparticles influence the rate of convection heat transfer since the surface are for the thermal transportation depends on these two factors. Moreover, cluster formation due to intermolecular attractive forces also results in heat transfer escalation. However, it can also result in sedimentation of nanoparticles [9].

Heat transfer mechanism is somewhat different in case of stationary nanofluid as compared to the moving nanofluids. In stationary nanofluid, mode of heat transfer is mainly conduction heat transfer. In conduction heat transfer , following mechanism of thermal transportation are mentioned in the literature [10].

- Brownian motion
- Nanoparticles clustering
- Nano layering effect
- Thermo-phonetics effect
- Ballistic transport and nonlocal effect
- Near field radiation.

However, convection heat transfer rate is increasing with moving nanoparticles in fluid. Convection heat transfer mechanism involves following critical factors that influence the performance of the fluid.

- Heat transfer surface area.
- Flow rate.
- Channel geometry.

Increase in surface area increases the heat transfer rate of the system. Nanoparticle size, cluster formation and nanoparticle volume fraction increases the surface area [11].

Increasing the flow rate increases the rate of heat transfer as it increases the interaction between molecules and particles. Flow rate increment increases the thermal transportation rate by increasing the turbulence inside the fluid [12].

Since the channel surface and geometry are in direct interaction with the heat transfer rate, these parameters have a critical importance in increasing the heat transfer. These parameters are frequently used in studies to increase heat transfer rate[13].

1.2.3. Thermophysical Properties of Nanofluids

Most important characteristics of nanofluid have been presented in (Fig 1.4) [14].

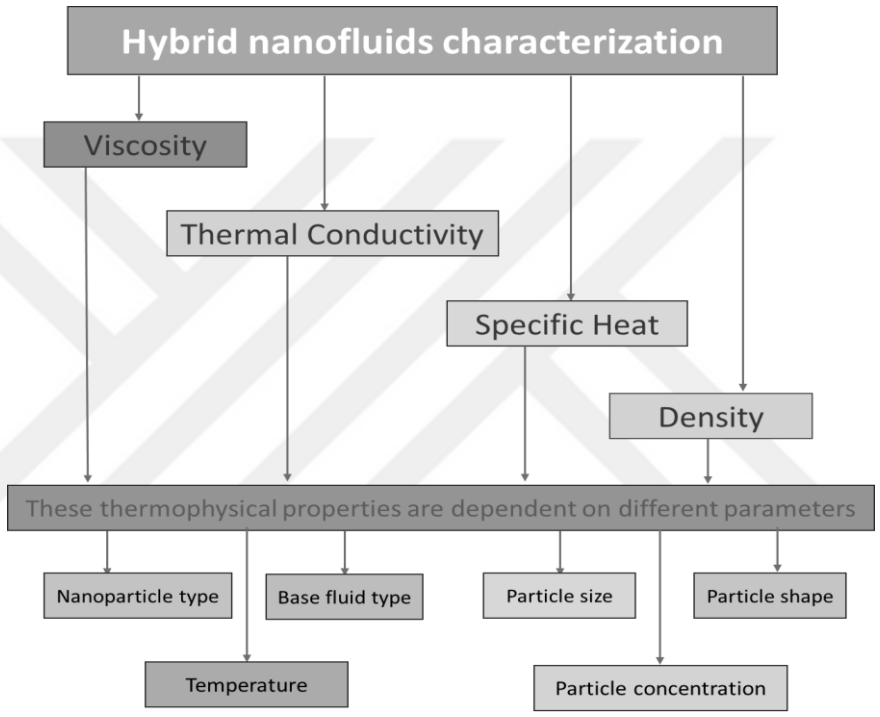

Figure 1.4. Nanofluid characteristics [14].

1.2.3.1. Thermal Conductivity

Superiority of nanofluids over the conventional fluids is due to higher thermal conductivity. Higher thermal conductivity of nanofluid is due to the presence of metallic nanoparticles. Thermal conductivity escalation is credited to the increased Brownian motion of nanoparticles in the base fluid [14]. The parameters that influence the thermal conductivity of nanofluids include:

- Brownian motion of nanoparticles.

- Temperature of the nanofluid.
- Flow rate of the fluid.
- Base fluid properties.
- Concentration of nanoparticles.

Concentration of nanoparticles directly affects thermal ocnductivty of the nanofluid. Increasing the concentration increase the number of nanoparicles. In creased number of nanoparticles help in increased surface area for heat transfer as well. Increasing the nanoparticle extent increases the molecular internation which eventually improves thermal conductivity of the nanofluids. Effect of concentration on nanofluid thermal conductivity has been presented in (Fig 1.5) [15].

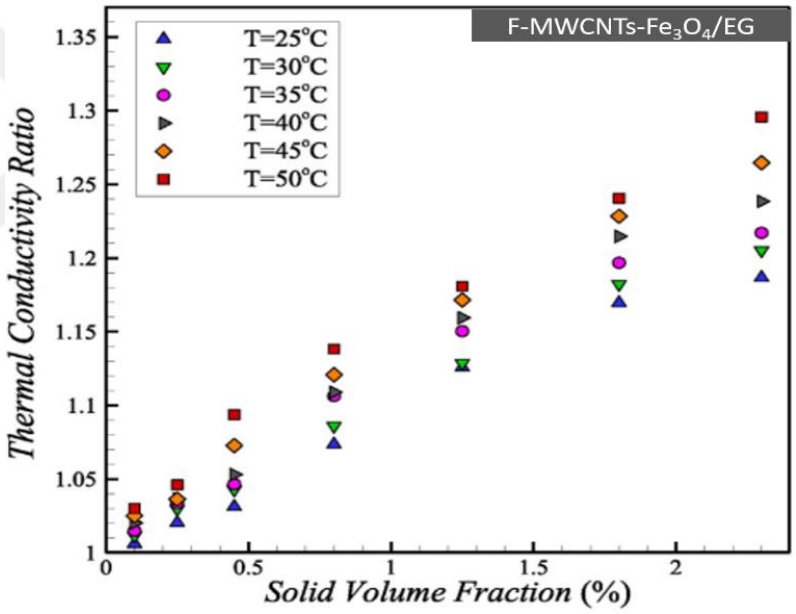

Figure 1.5. Influence of particle concentration on thermal conductivity of nanofluid [15].

Different base fluids depict different thermal conductivity escalation due to chemical interaction and competence as shown in Fig. 1.6 and Fig. 1.7 [15].

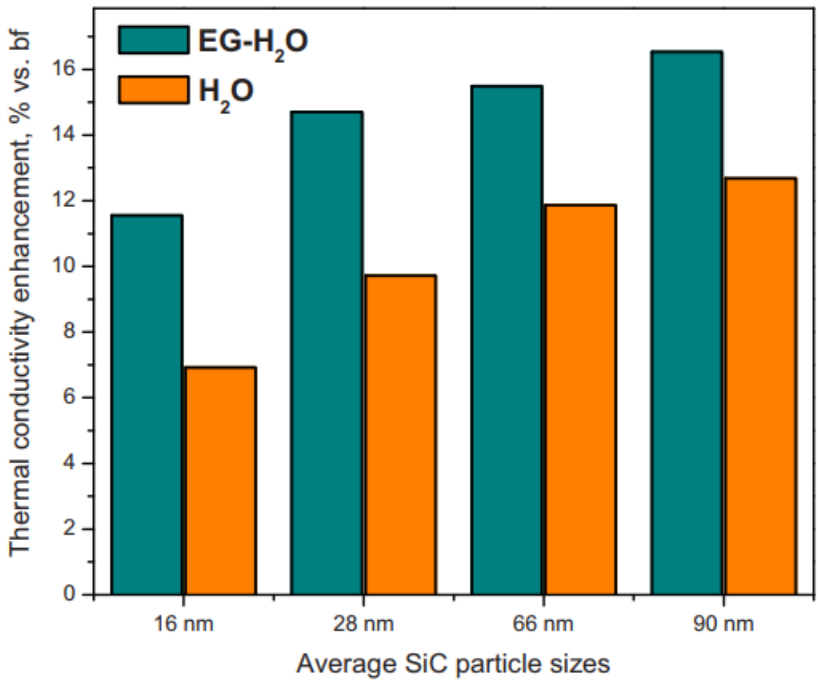

Figure 1.6. Effect of base fluid on thermal conductivity of the nanofluid [15].

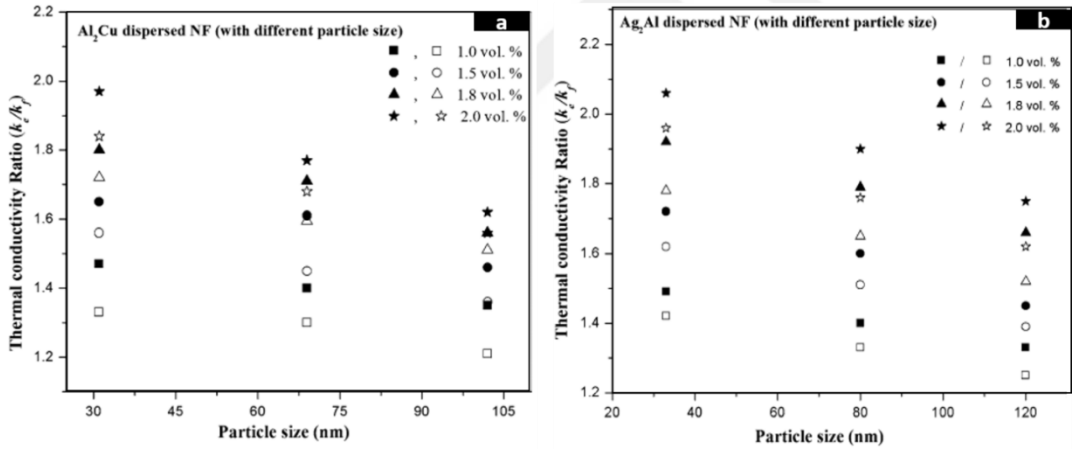

Figure 1.7. Influence of nanoparticle size on thermal conductivity of nanofluid [15].

Increase in temperature of the nanofluid also increase the molecular interaction which results in increased thermal conductivity as presented in Fig 1.8 [15].

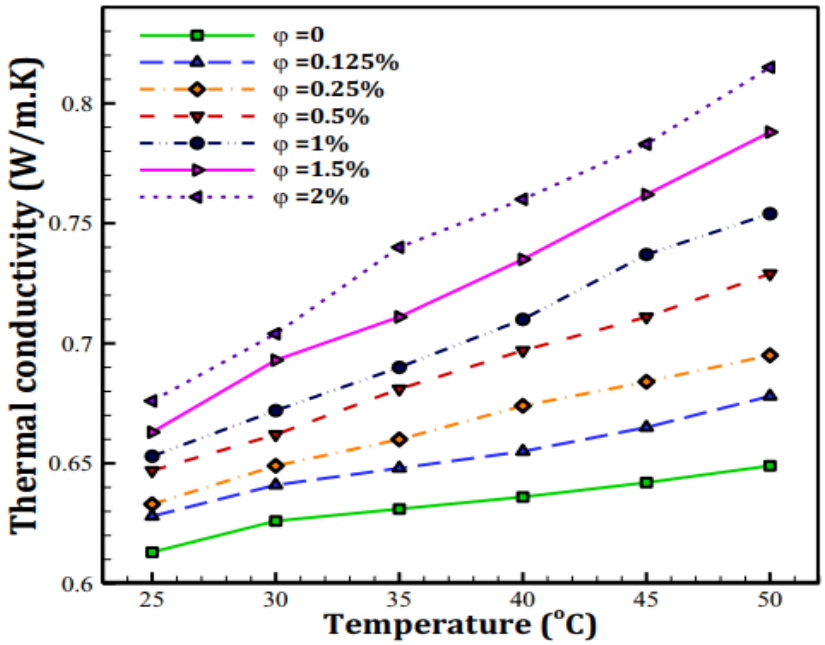

Figure 1.8. Effect of temperature on thermal conductivity o nanofluid [15].

Shape of nanoparticle also has significant effect on thermo-physical characteristics. Different shapes of nanoparticles have been presented in Fig 1.9 [15].

Shape	Name	Shape Factor (n)
Spherical		3.0
Platelet		5.7
Cylindrical		4.8
Blade/Laminar		16.2
Brick		3.7

Figure 1.8. Shapes of nanoparticles and shape factor value [15].

According to experimental studies, the thermal conductivity of carbon-based nanoparticles according to different shapes and concentrations are given in Fig 1.10. [16].

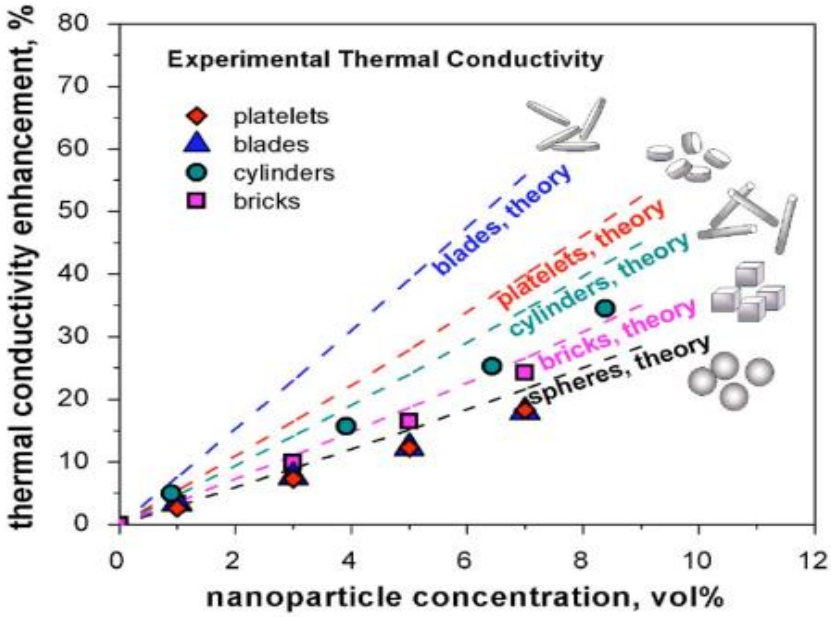

Figure 1.9. Nanoparticle shape effect on thermal conductivity of nanofluid [16].

1.2.3.2. Specific Heat

The specific heat (c_p) of the nanofluid can be increased or decreased with respect to the base liquid. It depends on the species, nanoparticle size concentration, temperature, and types of underlying fluids. If the place where the nanofluid is to be used has a rapid temperature change, it is possible to use a fluid with a low heat capacity in these places. The temperature changes as the specific heat of the most common nanofluids decreases as the fracture size and temperature increase.

If the specific heat of the nanoparticles is lower than the base liquid, then the specific heat of the nanofluid will decrease, for example the specific heat of Al_2O_3 nanoparticles is lower than that of water, so Al_2O_3 - water has a lower heat capacity than the base liquid. Which affects the specific heat of the nanofluid. So to get the required specific heat from the nanofluid we need to mix the appropriate

nanoparticles in the base fluid with the right volume concentration and temperature [17].

1.2.3.3. Density

The thermo-physical properties of nanofluids are influenced by many factors such as the nanoparticle size and nanoparticle shape, temperature, properties of the nanoparticles and the underlying liquid, particle aggregation, nanoparticle type etc.

Density is an important property that determines the effectiveness of nanofluids in heat transfer enhancement applications. Thus, accurate prediction of effective density becomes unavoidable for calculating the heat transfer coefficient of nanofluids. However, the change in density is directly related to the pressure drop, which is used to determine the pumping power for the developing flow. Density increases with increasing particle size and decreases with increasing temperature [18].

Experimental studies shows that the effect of the nanofluid density is a function of the temperature, the volume fraction of the nanoparticle, the density of the base fluid, and the ratio of the density of the base fluid to nanoparticles [19].

1.2.3.4. Viscosity

Nanofluid is a general name given to the fluids obtained by adding nanoparticles to the base fluid. Nanoparticle changes the physical properties of the base fluid including the thermal conductivity and viscosity. In the studies aimed at improving the heat transfer, firstly, millimeter and micrometer particles were added to the base fluid to improve the thermal properties of the working fluid. These fluids have brought along many problems such as congestion, precipitation and high pressure drop in the channel. In the continuation of the studies, in 1995, Choi added nanoparticles in the base fluid and invented the nanofluid. A significant increase in the thermal conductivity of the fluids was observed. Most of metal particles have a higher thermal conductivity than liquids, therefore adding a metal particle to the base fluid improves the convective transfer heat rate.

Many numerical and experimental studies have been carried out to determine the parameters that determine the thermal conductivity and viscosity of a nanofluid. Such parameters like volume ratio of nanoparticles, size and shape of nanoparticles, surfactants, temperature, different base fluid and using a hybrid nanofluid were investigated. The study examining the effect of changes in these parameters on viscosity is less than other studies in the literature. The random movement of particles and base fluid molecules in the nanofluid is directly related to the viscosity of the nanofluid. The viscosity value is very important for the pumping power of the nanofluid. The increase in pumping power will cause us to spend more energy. Therefore, we want the increase in heat transfer amount to be inversely proportional to the increase in pumping power.

The dynamic viscosity value of nanofluids is generally higher than the base fluid, and the dynamic viscosity value increases as the nanoparticle volumetric ratio increases. In the literature, it has been observed that the dynamic viscosity value of the nanofluid increases with the nanoparticle volumetric ratio, and as a result, the pressure drop and friction coefficient also increase. The dynamic viscosity value of the nanofluid is inversely proportional to the temperature. Nanofluid behaves non-Newtonian for higher nanoparticle volume ratio and exhibits Newtonian behavior for the lower nanoparticle volume ratio [20,21]. Changing the nanoparticle volumetric ratio and temperature are the parameters frequently encountered in the literature. Apart from this, nanoparticle size, nanoparticle shape, dispersion method studies are being investigated to determine the viscous effects of the flow, albeit less in number[22].

For viscosity calculations, different relationships [23–30] have been developed depending on parameters such as volume ratio and temperature. Empirical correlations were obtained with the data obtained as a result of the experimental studies. The results obtained are specific to the type of nanofluid and cannot be used in the case of different nanofluids or different nanoparticle sizes. Even there is dissimilarity in results of different studies on similar nanofluids. As a result of the studies, the nanoparticle size, shape, purity, preparation method, characterization

equipment, measuring methods, etc. were effective in the differences in the values [31].

In the literature about viscosity behavior of nanofluids reveals that although the presence of nanoparticles increases thermal conductivity of the base fluid. At the same time, the pumping power increases due to the increase in friction losses and pressure drop, and as a result, the operating cost increases. The viscosity of nanofluids is inversely proportional to temperature. However, as the temperature increases, the suspension stability of nanoparticles or the effect of surfactants decrease. Therefore, an increase in temperature can cause complications that are difficult to calculate.[32].

1.2.4. Potential Applications of Nanofluids

Owing to higher heat capacity value of nanoparticles, studies have been carried out for its use in many sectors. Nanofluids have been mainly studied for renewable energy applications and heat exchangers.

1.3. HEAT EXCHANGER AND HEAT SINKS

There are various types of heat exchanger. Some of the heat exchangers that have been used in the industry are:

- Flat tube heat exchangers.
- Plat type heat exchangers.
- Annular tube heat exchangers.

Flat tube heat exchangers have also been studied numerically and the model of such studies is shown in (Fig 1.11).

Heat sinks are using for cooling of electronic devices. Some of the types of heat sinks include:

- Micro channel heat sinks.
- Mini channel heat sinks.

Various geometries of fins have been designed for increasing convective heat transfer in heat sinks. Some examples of fin designs used in heat sinks are given below:

- Square fins.
- Pin fins.
- Wavy fins.
- Aero foil shaped fins.
- Rectangular fins.
- Triangular fins.
- Variable or Constant Area fins.
- Louvered fins.

Experimental setup of heat sinks for thermal management applications is shown in Figure 1.12 [33].

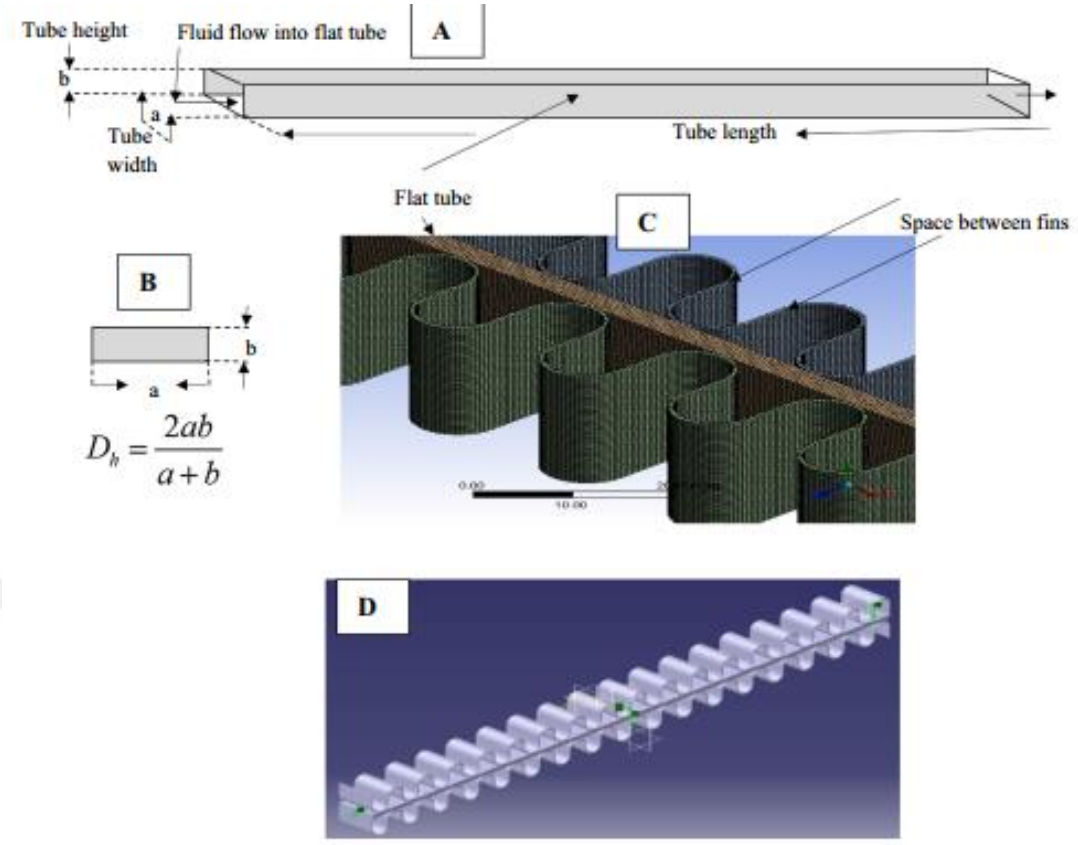

Figure 1.10. CAD model of flat tube heat exchanger [32].

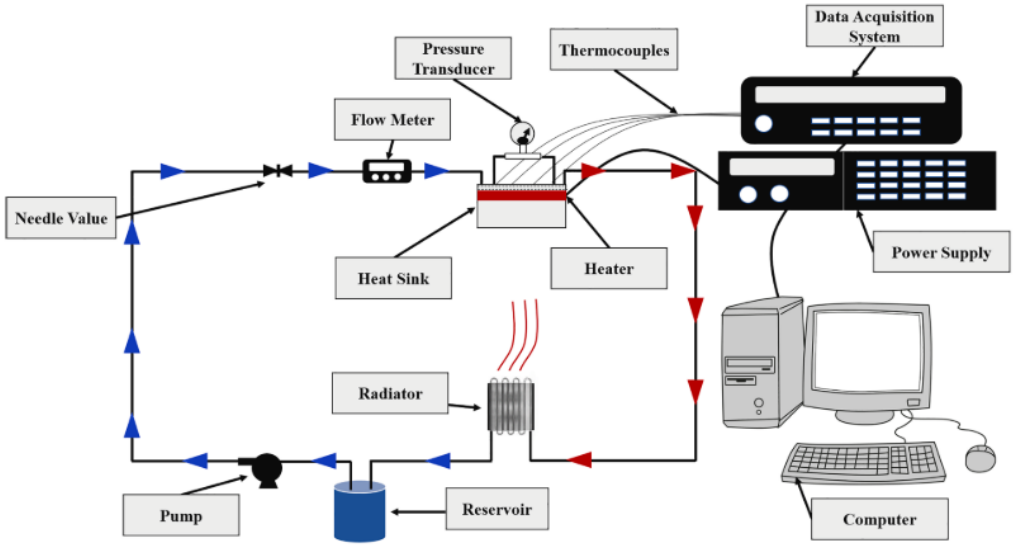

Figure 1.11. Example of heat sink experimental setup [33].

As can be understood from the literature, studies involving heat sinks are frequently encountered. In order to fill the gap in the literature, a heat sink design that is predicted to have higher heat transfer performance has been made and analyzed numerically.[34].

1.4. PROBLEM STATEMENT

In general, experimental studies are based on practical experiences in them on the use of various materials, devices, and equipment's. Also, scientific experiments requires a lot of time and effort, and sometimes it is also needed expensive equipment and supplies, and these materials are imported from any other country as well. Some studies needs a security clearance to carry out. We must add to this that the experimental studies often contained errors, forcing the researcher to start over with his research and instead repeat all the above. Numerical studies is frequently preferred today because it minimizes all these risks, and this study was carried out numerically for the same reasons. This study helps in understanding the heat behavior and flow of nanofluids in coiled conical tubes in heat transfer systems.

Numerical studies have been analyzed with using *ANSYS* Fluent software and reached results with almost zero error rate.

1.5. OBJECTIVES OF STUDY

The industrial development witnessed by humans and the interest in heat transfer systems in factories and various thermal systems. Coiled helical tubes have been used as a passive method for reaching higher convective heat transfer rate. Biggest advantages of coiled helical tube are easy to manufacture and low in cost and while the surface area of heat transfer is large, it occupies less space in size compared to straight pipes so this study aims to:

- It is a numerical study based on the boundary conditions of an experimental study. Experimental and numerical results will be compared.
- In order to reach the solution as soon as possible, the optimum mesh structure and number will be determined.
- The heat transfer rate and pressure drop values at different flow rates in the conical helical tube will be obtained as a result of numerical analysis.

- The effect of the change in nanoparticle volume ratio and the use of different nanoparticle shapes on the pressure drop and heat transfer characteristics will be examined in detail.

1.6. SCOPE OF STUDY

In this study, flow and heat transfer characteristics in a coiled conical tube has been numerically analyzed. Water has been used as the base fluid and added Al_2O_3 nanoparticles with three different nanoparticle volume ratio (1.0%, 2.0% and 3.0%) and three different nanoparticle shapes (platelet, blade and cylindrical) for obtaining nanofluid. The studies were analyzed under laminar flow conditions ($1050 \leq Re \leq 2150$). The constant heat flux has been applied on the tube surface. As a result, the effect of nanoparticle volume ratio and particle exchange on heat transfer characteristics and pressure drop will be numerically investigate.

PART2

LITERATURE REVIEW

2.1. HEAT EXCHANGER

Heat exchangers are classified on the basis of different criterion. For instance, on the basis of direction of working fluids, they are classified as parallel flow/co-current heat exchangers, counter flow/counter-current heat exchangers, and cross flow heat exchangers. Similarly, on the basis of mechanism of heat transfer, the heat exchangers are classified as, recuperative heat exchangers, regenerative heat exchangers, and evaporative heat exchangers. Moreover, the other types of heat exchangers include finned and un-finned heat exchangers; condensers, evaporators, and boilers; single pass and multi-pass heat exchangers; shell and tube heat exchangers, etc. [35].

Various shapes of heat exchanger tubes are in practice now a days and U-shape is most common of them all. However, there is immense research work underway nowadays on designing and testing of novel shapes of heat exchanger tubes owing to the critical role they play during the process of heat transfer between the hot fluid and the coolant [35]. The type and sizing of heat exchanger are the two most important selection criterions for a thermal system. The tubes through which the fluids flow in a heat exchanger are of critical significance. The most important aspects of a heat exchanger tube are presented in Fig 2.1. Geometry/shape of the heat exchanger tubes holds momentous significance in terms of design and manufacturing process and cost. Some of the common geometries of heat exchanger tubes that are in practice these days include flat tubes that have louvered fins attached [36], U-shape tubes, spiral tubes, etc. Physical appearance of most common Heat exchanger tubes is presented in Fig 2.2.

Nanofluids due to their idiosyncratic characteristics and thermal potential for heat exchanger applications have been vastly tested both numerically and experimentally. Encouraging results have been published and more research to obtain optimal design and operational parameters is underway. Many research groups and laboratories are involved with the nanofluids related projects [36].

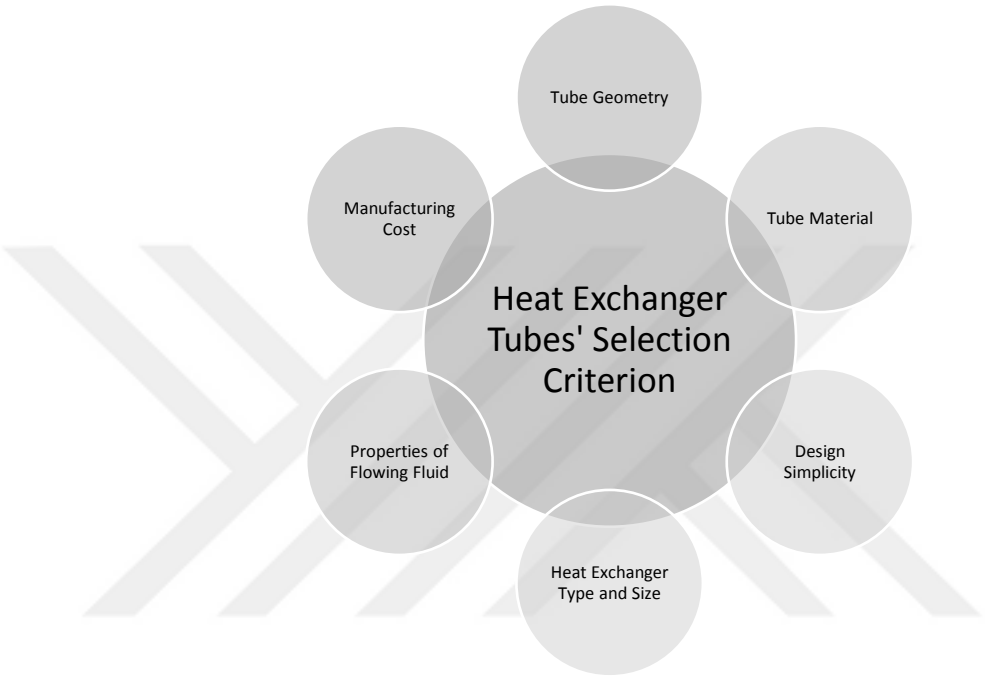

Figure 2.1. Selection criterion of heat exchanger tubes [36].

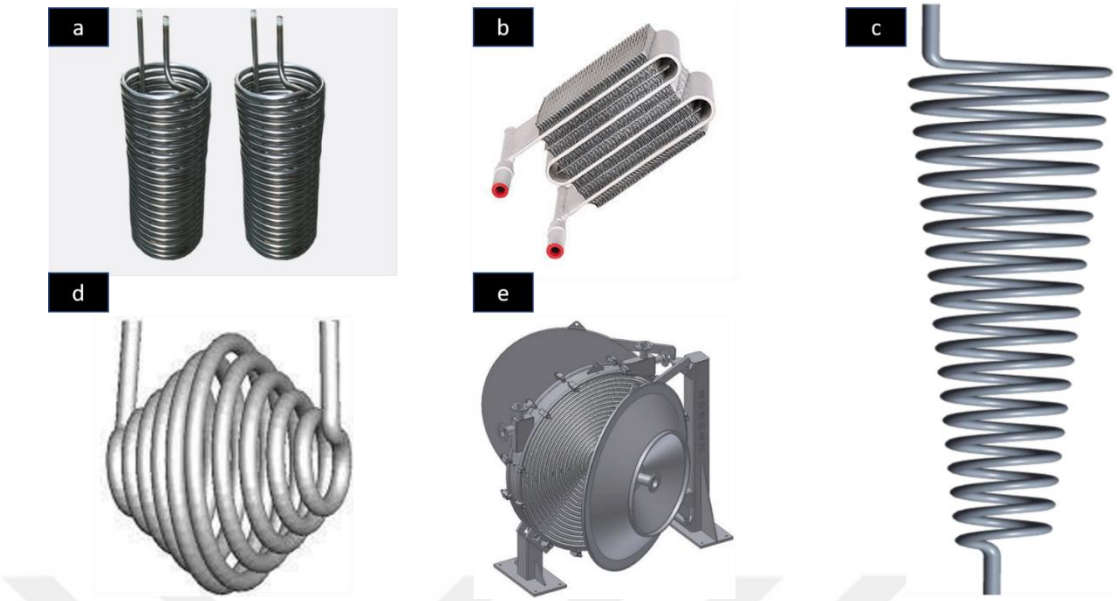

Figure 2.2. Geometries of heat exchangers, (a) Helical tube, (b) Flat tube, (c) Conical tube, (d) Spiral tube with varying curvature and (e) Spiral tube [36].

2.2. POTENTIAL OF NANOFLUIDS FOR HEAT EXCHANGERS

2.2.1. Nanofluids Performance in Flattened Tube Heat Exchangers

Experimental setup and schematic diagram for flat tube radiator heat exchanger shown in Fig 2.3. Nanofluids have been analyzed for different of heat exchangers. Shah et al. [36] tested water based silica (SiO_2-water) nanofluids for automotive radiators made of aluminum. It has 31 flat tubes with 32 louvered fins. Parameters of this study are 0.04-0.12% nanoparticle volume ratio, 60-70 ℃ inlet temperature, and 12-18 *LPM* flow rate. As a result of the study the amount of heat transfer increased by 36.92% at most shown in Fig 2.4. The fluids used in the experimental study were analyzed again after 3 days at the same boundary conditions and the difference due to precipitation was observed as 1.0 %. In addition, as a result of the study, it was observed that the inner surface of the pipes deteriorated due to the rapid temperature change that caused the thermal cycles to intensify the local thermal stress. Abbas et al. [8] analyzed Fe_2O_3-TiO_2/water hybrid nanofluid in flat tubes with louvered fins and found out that the use of nanofluids increased the *Nu* in the flat tubes by 20.03% as compared to the base fluid. Parameters are 0.005-0.009 % nanofluid volume ratio, 48-56 ℃ inlet temperature and 11-15 *LPM* flow rate. [8].

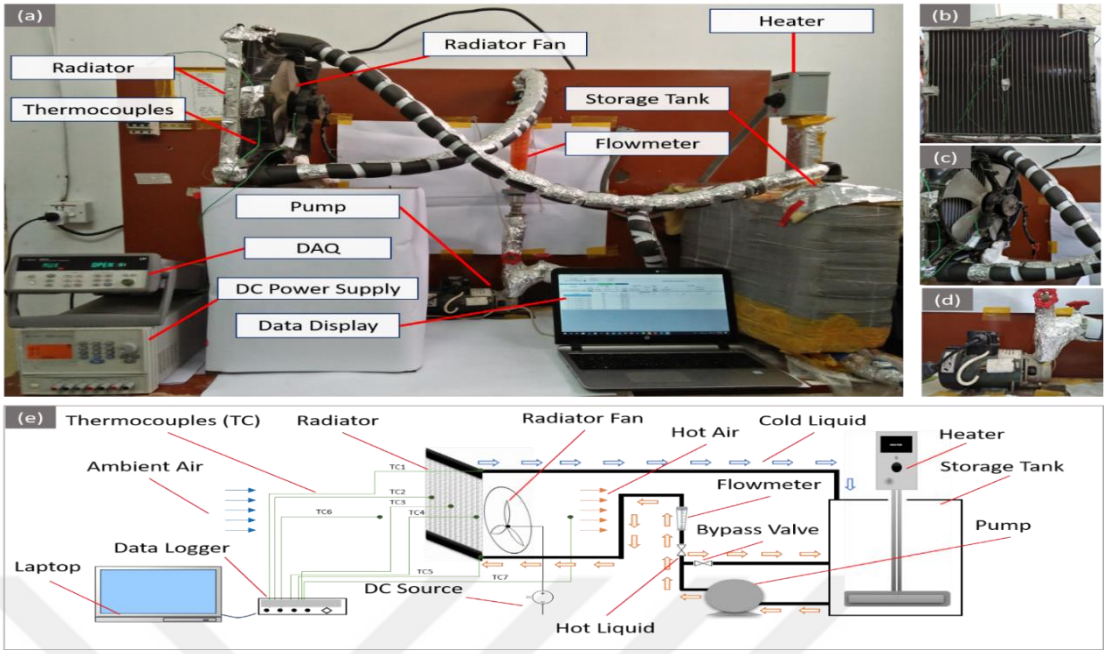

Figure 2.3. Nanofluids test setup for flat tube radiator heat exchanger (a) Experimental setup and (b) Schematic diagram [36].

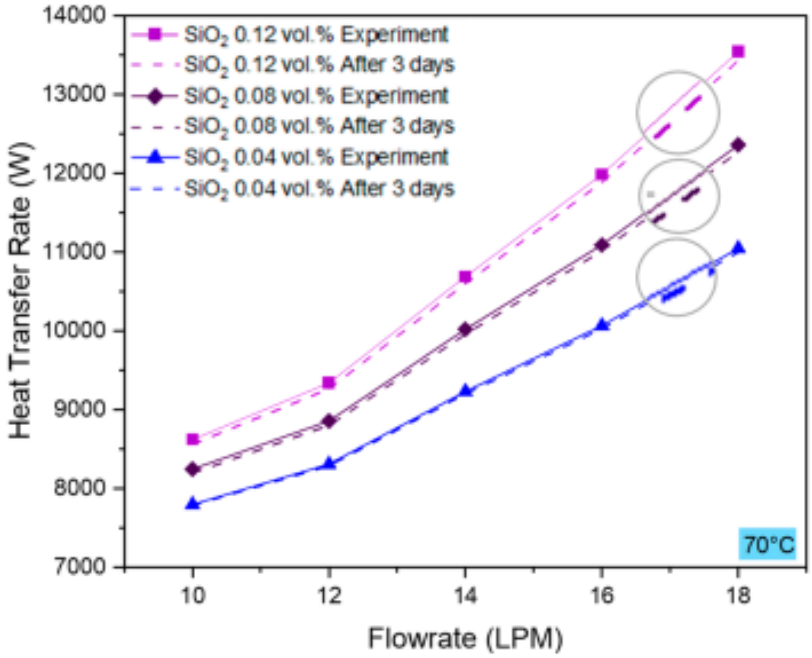

Figure 2.4. Repeatability tests for heat transfer rate after 3 days of initial testing [36].

Vajjha et al. [37] numerically analyzed on heat transfer and fluid dynamic performance evaluation of CuO and Al_2O_3 based nanofluids in flattened tube. Al_2O_3 and CuO nanoparticles of concentration 0.05%, 0.15% and 0.3% have been added to

the base fluid and then evaluate the heat transfer characteristics of the nanofluid. The mass flow rate of nanofluid in the flat tube has been kept constant. It has been observed that the nanofluid that exhibited the highest heat transfer performance was The CuO nanofluid. The heat transfer rate increased by 89% as compared to the base fluid for using CuO based nanofluid at 0.3 vol.%. As a result of the study, it was determined that the increase in the Reynolds number had a greater effect on the heat transfer rate than the increase in the nanoparticle volumetric ratio. Elsebay et al. [38] also numerically appraised the performance of CuO and Al_2O_3 nanofluid with water as base fluid and varied the concentration of nanoparticles from 1 vol.% to 7 vol.% in 250-1750 Reynolds number range. The focus of their study was the resizing or miniaturization of radiator with increased heat transfer owing to superior thermal characteristics of nanofluids over the water. heat transfer coefficient enhancement reached up to 45% and 38% for Al_2O_3 nanofluid and CuO nanofluid, respectively. Alumina based nanofluid can enable higher reduction in length of the tube as compared to CuO based nanofluids. Yahya and Saghir [39] numerically studied the performance of Al_2O_3/water nanofluids in flat tube radiator and observed 12% heat transfer escalation at 2 vol.% of nanofluid as compared to the water, whereas the enhancement was 5% at 1 vol.% concentration of nanoparticle. Erdogan et al. [40] appraised entropy generation and energy performance of Al_2O_3/EG-water nanofluid in flat tube radiator at 95 ℃ inlet temperature and flow rate of 10-20 *LPM* flow rate. Air velocity was varied from 4 to 5 *m/s.* They reported 9.52% increment in heat transfer rate 4 m/s velocity of air nanofluid flow rate of 10 *LPM*. They reported an increase in pressure drop for the nanofluids however overall performance index was reported to increase by 18.8% at 4 m/s velocity of air. Ahmed et al. [41] evaluated improvement in thermal performance of flat tube car radiator by using TiO_2/water nanofluid. The tested nanoparticle range was 0.1 – 0.3 vol.%. They reported 47% improvement in effectiveness of radiator due to the use nanofluids. Sundari et al. [42] appraised the performance of car radiator using Al_2O_3/glycerin nanofluid. The volume concentration was varied in the range of 0.1-0.3 vol. % and an enhancement of 54.56% in heat transfer was reported along with 90% effectiveness of radiator at 0.3 vol. % and 1500 Reynolds number. Said et al. [43] also appraised thermal performance of automotive radiator by using Al_2O_3 and TiO_2 nanoparticles based nanofluids with EG-water base fluid. They reported 24.21% improvement in Nu

performance of radiator as compared to the base fluid when 0.3 vol/% of nanoparticles was dispersed in base fluid. Jadar et al. [44].

Tested *f*- MWCNT/water nanofluid for automotive cooling system and observed 45% enhancement in heat transfer rate as compared to the base fluid. Bejjam et al. [45] performed *CFD* analysis of the performance of water, EG-water, and 0.05-0.2 vol.% Al_2O_3 nanofluids in automotive radiator. Utmost increment of 10.64% in Nu 3.82% in heat Transfer coefficient. Major findings of some of the recent studies published between 2016 to 2022 have been reported in table 2.1 [43].

Careful analysis of table 2.1 reveal that nanofluids depict promising potential as a coolant in flat tube heat exchangers. Performance of nanofluids in flat tubes are influenced by the temperature of fluid, flow rate of the fluid, concentration of the nanoparticles in the base fluid, and size and shape of the nanoparticles. Increase in Reynolds number is mostly reported to hike the thermal performance of the system. Increase in flow rate enables the nanofluids to exchange heat at higher rate because of turbulence effect. Increase of temperature also results in improved heat transfer rate since the temperature increase increases the Brownian motion of nanoparticles. higher temperature however causes the surface deterioration of the channels/tubes [46].

Moreover, the concentration of nanoparticles also manifests critical effect. Increase of concentration is recorded to increase the performance however, there is an upper limit of concentration of nanoparticles depending on the nanoparticle type, base fluid type and the operational conditions. Beyond the upper limit the performance tends to depreciate. The performance depreciation due to increased number of nanoparticles occurs because the nanoparticles tend to agglomerate and sometimes the clogging in the channels starts to occur [47].

Although most of the studies report positive impact of using nanofluids in the heat exchangers however, some of the studies also report the otherwise results. Therefore, there is an imperative need to conduct further research to draw conclusive understanding of the nanofluid performance phenomenon [48].

2.2.2. Nanofluid Performance in Helical Tube Heat Exchangers

Various shapes of helical tubes for heat exchanger are in practices for heat transfer intensification. Simple helical tubes are of uniform area of curvature however, there are other helical tubes as well with variable curvature area as well. Another helical shape is known as conical shaped helical tube [49].

Huminic [50] studied heat transfer rate of nanofluids as compared to the base fluid in an counter flow double pipe helical tube heat exchanger (Fig 2.5) through *CFD* analysis . They tested TiO_2/water nanofluid and Cuo/water nanofluid. Concentration of nanoparticles was varied from 0.5 vol.% to 3 vol.%. Nanofluids were asset to flow through the inner tube and water was set to flow through the annulus. They observed 14% greater rate of heat transfer for 2 vol.% Cuo/water nanofluid flowing at same flow rate through inner tube and the annulus. Bahremand et al. [51] numerically and experimentally studied turbulent convection flow nanofluid flow in helical tubes. They observed greater heat transfer as well as higher pressure drop in the helical tubes. Kumar et al. [52] conducted *CFD* analysis of thermal and fluidic characteristics of MWCNT/water nanofluid in helical coil tube heat exchanger. They conducted the analysis in laminar regime and in the range of 1300-2200 Dean number, and the concentration was kept as 0.2, 0.4, and 0.6 vol.% of nanoparticles. They reported 30% enhancement in Nu for 0.6 vol.% of nanofluid at 1400 Dean number. Moreover, at 2200 Dean number, the pressure drop reached up to 11% as compared to the base fluid. Radkar et al. [53] performed detailed experimentation to evaluate thermal potential of nanofluids in helical tubes of heat exchanger using ZnO/water nanofluid. They obtained 18.6% enhancement in Nu for 0.25 vol. % concentration of nanoparticles in the base fluid. They associated the anomalous augmentation in thermal performance of nanofluids to the tube geometry that makes the effectiveness of heat exchanger quite significant. Singh et al. [54] examined the performance of CNT/water nanofluid in helical tube heat exchanger and they observed a momentous elevation in overall heat Transfer coefficient of 62.62% as compared to the base fluid. They also reported an increase in thermal conductivity of nanofluid of 162% when the surfactant-water base fluid was used. Whereas thermal conductivity escalation was 152% when the water had no surfactant. Kulkarni et al.

[55] tested the performance of silver/water nanofluid in helical coiled heat exchanger and they reported 32% elevation in heat Transfer coefficient as compared to the base fluid.

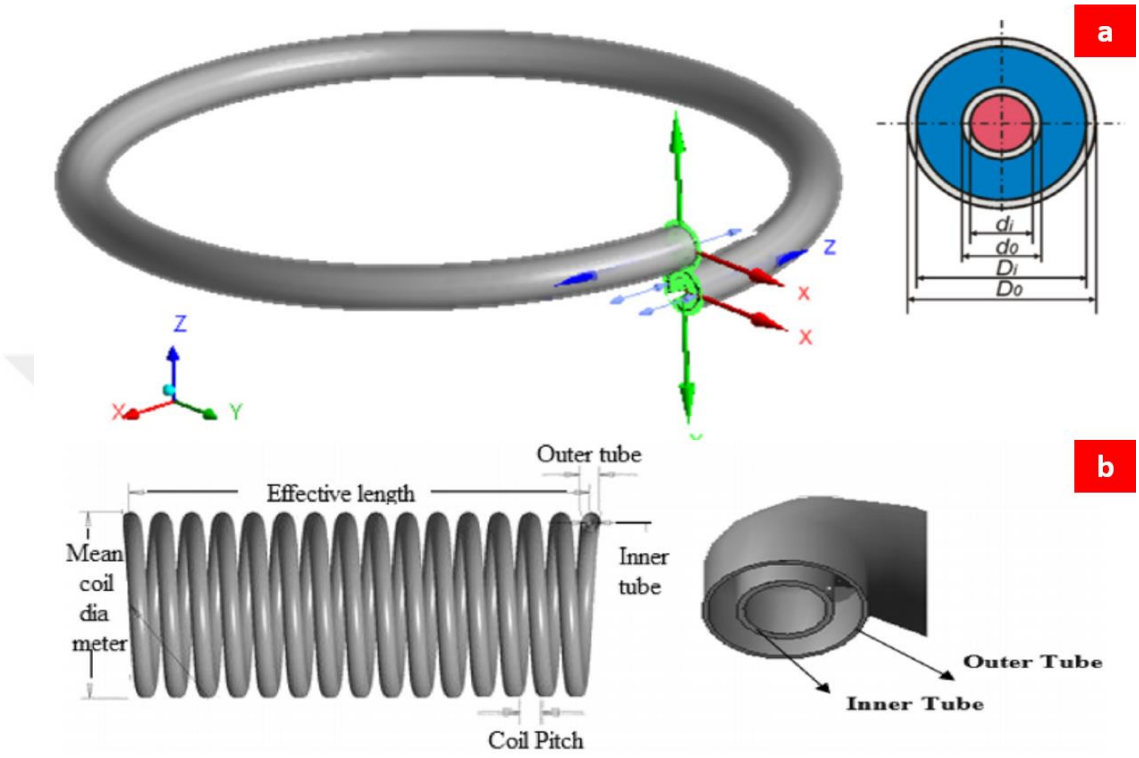

Figure 2.5. Geometry design of double pipe helical tube (a) Single section and (b) Full tube [55].

Set up to test the performance of helical tube heat exchangers is presented in Fig 2.6. Niwalkar et al. [56] appraised the performance of SiO_2/water nanofluid in helical tube heat exchanger with various nanoparticles loading ranging from 0.05 vol.% to 0.25 vol.% and the flow rate ranged from 30 LPM to 50 *LPM*. Presence of nanofluid increased the heat transfer coefficient by 28.71%. Bhanvase et al. [57] tested polyaniline (*PANI*) nano fiber based nanofluid having the nanoparticles dispersed in water. A concentration of 0.1-0.5 vol.% was tested. heat transfer coefficient was obtained to be 10.52% higher than the base fluid at 0.1 vol.% loading of nanoparticles. Whereas the enhancement reached up to 69.62% at 0.5 vol.% concentration of nanoparticles in the base fluid. Bahiraei et al. [58] evaluated the performance of Al_2O_3/water in helical tube heat exchanger they observed increment in heat transfer as well as pressure drop. Narrein and Mohammed [59] carried out

extensive numerical study on performance evaluation of Al_2O_3, SiO_2, Cuo, and ZnO based nanofluid in helical tube heat exchanger. The tested range of was 1-4 vole l% nanoparticle concentration, and 25-80 nm nanoparticles size range. They tested water, ethylene glycol, and engine oil as base fluids. Cu based nanofluids outperformed rest of the nanofluids in terms of Nu escalation. Convective heat transfer was reported to deteriorate past 2 vol.% concentration due to anomalous pressure drop that diminishes the overall effectiveness of nanofluids in helical tubes [59]. Major findings of studies on helical tube heat exchangers are presented in table 2.2.

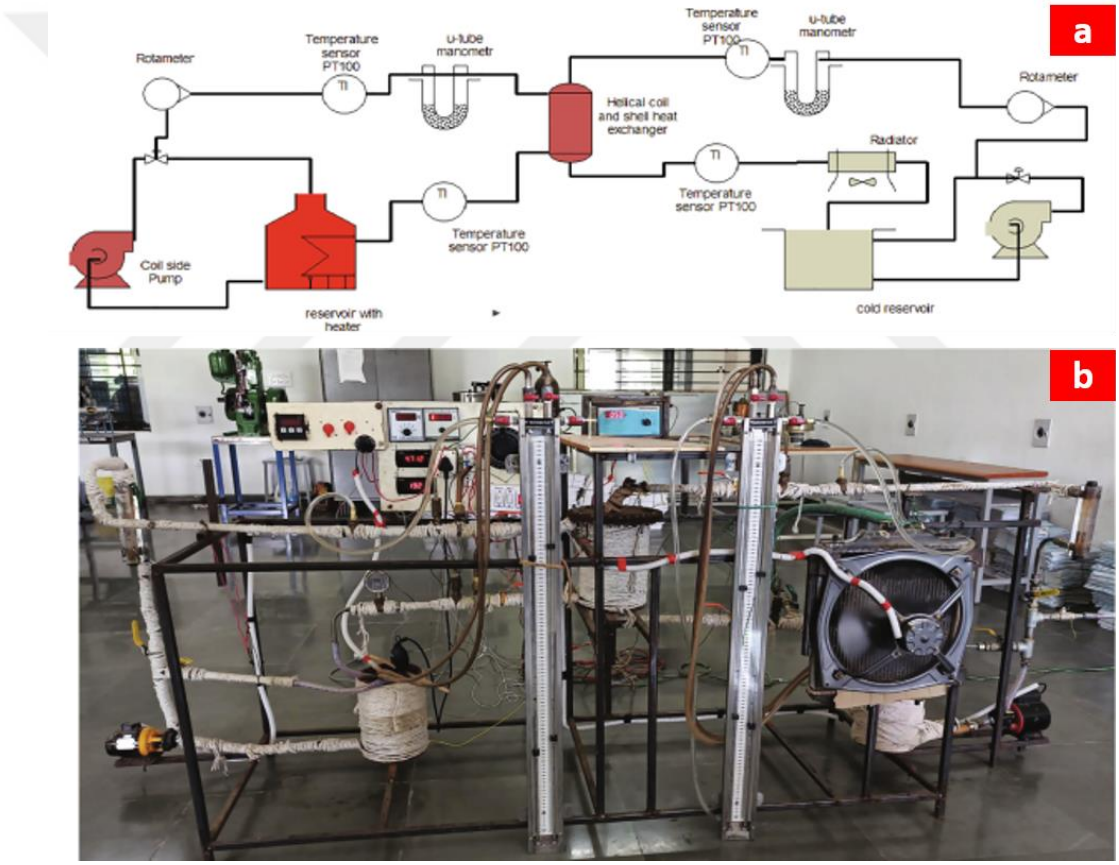

Figure 2.6. Test section arrangement for helical tube heat exchanger using nanofluid (a) Schematic representation and (b) Experimentation setup [59].

Zare and Hayht [60], carried out their studies by combining two passive techniques. Within these techniques, coiled tubes and CuO-water nanofluid were used to improve heat transfer. Constant wall temperature was applied in all studies. The thermo-physical properties of the fluid have also been used as temperature-dependent functions. While Brownian effects were adopted in the thermal conductivity and dynamic viscosity of the nanofluid. The results and experimental data were verified numerically, the samples were drawn using AutoCAD version 2015 and the governing equations were solved numerically using computational fluids as showing in Fig 2.7 and Table 2.1. For the heat transfer coefficient and pressure drop in the coiled spiral tube of different Reynolds numbers. This study was conducted on four tubes. The first is a cone-shaped coiled tube and the other tubes are spiral coiled tubes and have lower, normal and higher diameters as showing in Fig 2.8.

The velocity profiles indicated stronger secondary flow in conical coiled tube at a specified Dean number. The obtained results also showed higher heat transfer enhancement in the conical coiled tube in comparison with helical coiled tube with the same average pitch coil diameter. Moreover, the nanoparticle-induced heat transfer enhancement was more effective in conical coiled tube. [60].

Table 2.1. Computational grids.

Tubes	Number of Elements
1	345,200
2	517,900
3	544,300
4	776,100

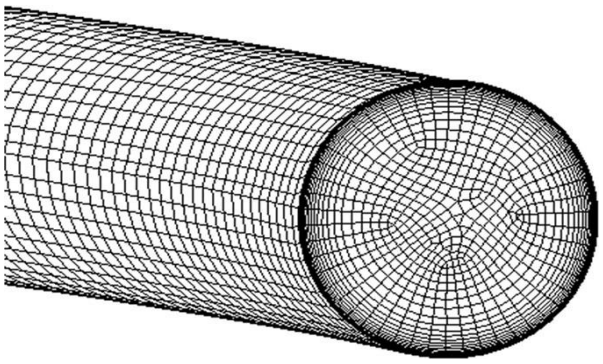

Figure 2.7. Computational domain [60].

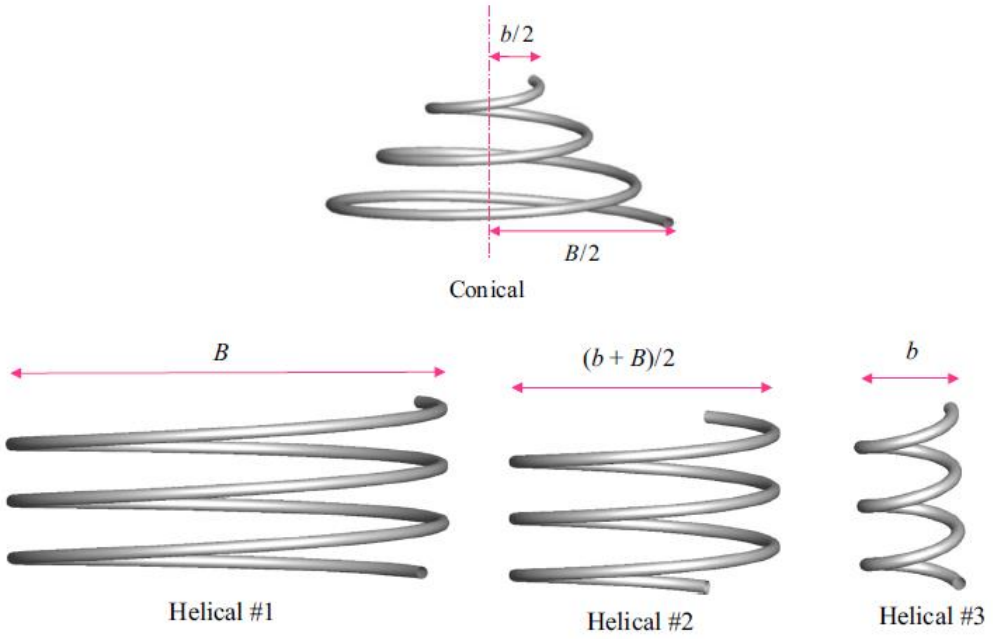

Figure 2.8. Schematic of helical tubes and conical helical tube [60].

Mahdi. et al. [61] studied heat and hydrodynamic transfer of water and SiO_2/water flow in conical coiled tubes. The experimental platform was set up as shown in Fig 2.9.

The heat transfer and pressure drop of fluid flowing under fixed wall conditions were studied in coiled conical tubes in order to better understand fluid flow physics, thermal conductivity and fluid dynamics, and all experimental steps were performed experimentally.

The results showed in this study Heat transfer increased by 26% and pressure decreased by 117%. Reducing the angle of the coiled conical tube increases heat transfer with decrease in pressure, changing the angle of the coiled conical tube is more effective than changing the diameter of the base circle in the coiled conical tube [61].

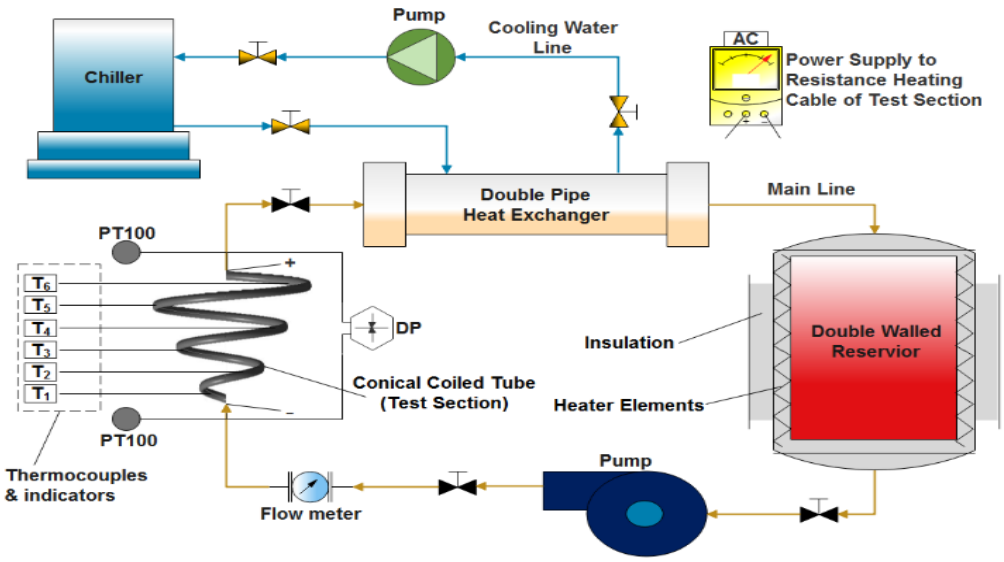

Figure 2.9. Illustration of the experimental platform and how it works [61].

Altunay [66] numerically investigated the flow of Al_2O_3-water nanofluids with different nanoparticle shapes in the serpentine microtube. Study included many different parameters. These were different Reynolds numbers ($750<Re<2000$), different nanoparticle shapes, different nanoparticle volume ratio (1.0%, 2.0%, and 3.0%) and different channel lengths. In the study, constant heat flux was applied to the Channel surface. A serpentine micro tube with a step of 10 mm, a diameter of 787 µm, and a length of 30 mm was used in the study as shown in Fig 2.10.

The average Nusselt numbers and the average Darcy friction factors were used to estimate the flow and heat transfer performance in the serpentine micro tubes. The results of the study are obtained for 1.0%, 2.0%, 3.0% nanoparticle volume fractions and different nanoparticle shapes. Velocity and temperature distribution inside the micro tube were also examined for different cases. Secondary flows in serpentine As the variation of average Nusselt number as showing in Fig 2.11 and Darcy friction factor with Reynolds number, nanoparticle shape and nanoparticle volume fraction. As a result, the highest convective heat transfer performance was obtained for platelet nanoparticle shape of the %3.0 Al_2O_3-water nanofluid [66].

Since in our study the same nanofluid and the same nanoparticles with water were used as the base liquid.

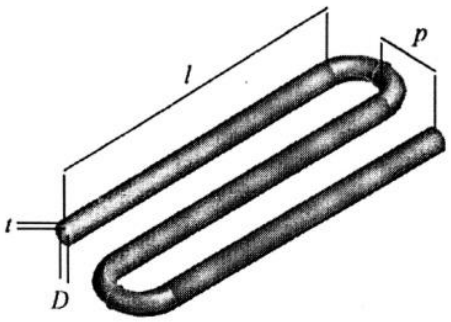

Figure 2.10. Technical appearance of the model [66].

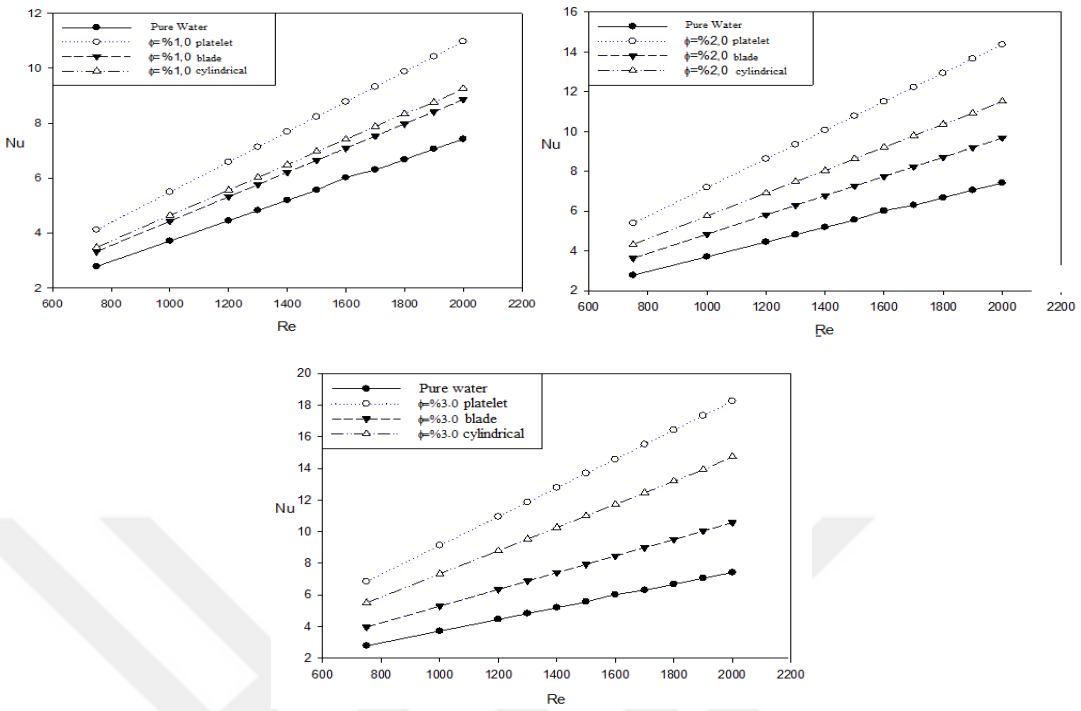

Figure 2.11. Effect of nanoparticle shape change on average Nusselt number for 1.0%, 2.0% and 3.0% nanoparticle volumetric ratio, respectively [66].

Major findings of some of the recent studies on nanofluids in heat exchangers are listed in Table 2.2.

Table 2.2. Major findings of some of the recent studies on nanofluids in heat exchangers.

Reference	NF	Tube Geometry	Major Findings
Vajjha et al. [37]	CuO and Al_2O_3 based nanofluids	Flat Tube	94% enhancement in heat transfer rate at 2000 Reynolds number and 10 vol. % concentration of Al_2O_3 nanofluid over the base fluid. The heat transfer rate increased by 89% as compared to the base fluid for Cuo based nanofluid at 6 vol. %.
Elsebay et al. [38]	CuO and Al_2O_3 based nanofluids	Flat Tube	Heat transfer coefficient enhancement reached up to 45% and 38% for Al_2O_3 nanofluid and Cuo nanofluid, respectively.
Yahya and Saghir [39]	Al_2O_3 based nanofluids	Flat Tube	12% Heat transfer escalation at 2 vol. % of nanofluids as compared to the water, whereas the enhancement was 5% at 1 vol. % concentration of nanoparticles.
Erdogan et al. [40]	Al_2O_3/EG-water	Flat Tube	They reported 9.52% increment in heat transfer rate 4 m/s velocity of air nanofluids flow rate of 10 LPM. They reported an increase in pressure drop for the nanofluids however overall performance index was reported to increase by 18.8% at 4 m/s velocity of air.
Ahmed et al. [41]	TiO_2/water	Flat Tube	47% improvement in effectiveness of radiator due to the use nanofluids.
Sundari et al. [42]	Al_2O_3/glycerin	Flat Tube	The volume concentration was varied in the range of 0.1-0.3 vol. % and an enhancement of 54.56% in heat transfer was reported along with 90% effectiveness of radiator at 0.3 vol.% and 1500 Reynolds number.
Said et al. [43]	Al_2O_3 /EG-water and TiO_2/EG-water	Flat Tube	24.21% improvement in Nu performance of radiator as compared to the base fluid when 0.3 vol/% of nanoparticles was dispersed in base fluid. Alumina based nanofluids outperformed the titanium based nanofluids.

Reference	NF	Tube Geometry	Major Findings
Jadar et al. [44]	*f*-MWCNT/water	Flat Tube	Observed 45% enhancement in heat transfer rate as compared to the base fluid.
Bejjam et al. [45]	Al_2O_3 NFs	Flat Tube	Utmost increment of 10.64% in Nu 3.82% in heat transfer coefficient.
Selvam et al. [62]	Graphene/EG-water	Flat Tube	A range of 0.1-0.5 vole l.% concentration, 10 g/s – 100 g/s flow rate of nanofluid, and inlet temperature of 35 ℃ and 45 ℃ was tested. They reported 20% enhancement in CHTC for 0.5 vole %, 100 g/s and 35 ℃ inlet temperature. An increment of 51% in CHTC at 0.5 vol.%, 100 g/s and 45 ℃ inlet temperature was reported.
Goudarzi and Jamali [63]	Al_2O_3 /EG	Flat Tube with Wire Coil Inserts	An increment of 5% in thermal performance for nanofluid based system of coil inserts was reported.
Rai et al. [64]	MgO/EG-water	Flat Tube	Flow rate and nanoparticle concentration augmentation was concluded to be the major cause of heat transfer performance intensification. Percentage of heat transfer augmentation increases from 5.59% to 29.83% when the nanoparticle concentration increases from 0.1 vol.% to 0.2 vol.%.
Li et al. [65]	SiC-MWCNT/EG	Flat Tube	Topmost augmentation in heat transfer coefficient was 26% at 0.4 vol.% concentration.
Choi et al. [66]	Al_2O_3 /EG-water	Round Tube	6.9% increase in heat transfer rate was reported.
Kahani et al. [67]	CuO/EG-water	Shell and Tube	Reynolds number increment increased the thermal performance of the nanofluid based system.
Soylu et al. [68]	Cu and Ag dopped TiO_2/EG-water	Flat Tube	Maximum increment in CHTC was reported to be 26.15% for 1 vol.% concentration and an increment of 27.72% was reported at 2 vol.% concentration of NF.
Safikhani et al. [69]	Al_2O_3/water	Flat Tube	Increase in heat transfer was reported.
Safikhani et al. [70]	Al_2O_3/water	Flat Tubes with Multiple Tapes	heat transfer and friction factor increased by 50% and 220% respectively.

Reference	NF	Tube Geometry	Major Findings
Ramalingam et al. [71]	Al_2O_3-SiC/EG-water	Flat Tube	Maximum increase of 28.34% in overall thermal performance was observed at 0.8 vol.% of NPs in the base fluid.
Guo et al. [72]	Al_2O_3 /water	Flat Tube	Topmost augmentation in heat transfer was reported to be 11.1%. Average pressure-drop at maximum tested NP concentration of 0.5 vol. % increased by 4.4%.
Sharma et al. [73]	CuO/water	Flat Tube	An increase of 6.75% in Nu and 14% in heat transfer coefficient was reported at 50 ℃ temperature and 9000 Reynold number.
Alirezaie et al. [74]	MgO/water Ag/water MWCNT/water DWCNT/water	Flat Tube	Topmost increment in heat transfer was reported to be 50% and the efficiency range was 10-40%. MWCNT based nanofluid outperformed rest of the nanofluids.
Sun and Liu [75]	CuO/water and Al_2O_3/water	CPU Radiator	Nanofluid concentration range was 0.1-0.5 vol.% and the Reynolds number range was 400-2000. Convective eat transfer coefficient of Cuo/water based nanofluid was 1.1-2 times higher than the base fluid.
Oliveira et al. [76]	MWCNT/water	Flat Tube	They reported 5% decrease in heat transfer rate.
Kumar et al. [77]	Al_2O_3 /water ZnO/water CuO/water	Flat Tube	Greatest increment in heat transfer coefficient was reported to be 42.5%, 47.4%, and 51.1% for 2 vol.% Al_2O_3 /water, ZnO/water, and Cuo/water nanofluids, respectively.
Zhao et al. [78]	Al_2O_3 /water	Flat Tube	Convective heat transfer for nanofluid increased by 1.236 times as compared to the base fluid.
Abdolbaqi et al. [79]	TiO_2/Bio glycol-water	Flat Tube	Temperature ranged 30-70℃, concentration ranged 0.5-2 vol. %. Nu at 2 vol. % was 3% lesser than the base fluid. Nu increment approached 28.2% at optimum operational conditions.

Reference	NF	Tube Geometry	Major Findings
Kaska et al. [80]	AlN-Al_2O_3/water	Flat Tube	Maximum Nu values were achieved at 3 vol.% and the enhancement was about 50% as compared to the base fluid. However, the Nu enhancement was observed to dropped at 4 vol.% of nanoparticles. Moreover, heat transfer increased from 28% to 58% when the nanoparticle volume concentration increased from 1 vol.% to 3 vol.%. Whereas, at 4 vol.% concentration the heat transfer enhancement reduced to 33%.
Subhedar et al. [80]	Al_2O_3/EG-water	Flat Plate	Operation conditions were opted to be 0.2-0.8 vol.% concentration, 4-9 LPM flow rate, and 65-85 ℃ inlet temperature. At 0.2 vol. % concentration of NPs the heat transfer increased by 30%. At 0.8 vol. % concentration the Nu enhanced by 28.47% as compared to the base fluid.
Hussein et al. [81]	TiO_2/water	Flat Plate	1-4 vol. % concentration, 10,000-100,000 Reynolds number, 60-90 ℃ inlet temperature was tested. Nanoparticle Even at low concentration the efficiency improved by 20%.
Zhang et al. [82]	TiO_2/water	Flat Plate	Nu decreased with increasing nanoparticle concentration. However, the values were greater than the base fluid.
Elsaid [83]	Co_3O_4/EG-water Al_2O_3/EG-water	Flat Plate	Cobalt oxide based nanofluid outperformed aluminum oxide nanofluid in terms of thermal performance.
Tijani and Sudirman [84]	Al_2O_3/EG-water CuO/EG-water	Flat Plate	The values of observed Nus were 164.29, 193.19, and 208.71 for base fluid, 0.3 vol.% of Al_2O_3 nanofluids and 0.3 vol.% of Cuo nanoparticles, respectively.
Huminic and Huminic [85]	MWCNT-Fe_3O_4/water	Flat Plate	A decrease of 26.483% in entropy generation was observed for hybrid nanofluid as compared to the base fluid.
Ali et al. [3]	MgO/Water	Flat Plate	31% maximum increase in heat transfer was reported at 0.12 vol.%

Reference	NF	Tube Geometry	Major Findings
Ahmed et al. [86]	TiO_2/water	Flat Plate	Effectiveness increased by 47%
Chen and Jia [87]	TiO_2/EG-water	Flat Plate	10% enhancement in convective heat transfer occurred.
Reference	NF	Tube Geometry	Major Findings
Vajjha et al. [37]	Cuo and Al_2O_3 based nanofluids	Flat Tube	94% enhancement in heat transfer rate at 2000 Reynolds number and 10 vol. % concentration of Al_2O_3 nanofluid over the base fluid. The heat transfer rate increased by 89% as compared to the base fluid for Cuo based nanofluid at 6 vol. %.
Elsebay et al. [38]	Cuo and Al_2O_3 based nanofluids	Flat Tube	Heat transfer coefficient enhancement reached up to 45% and 38% for Al_2O_3 nanofluid and Cuo nanofluid, respectively.
Yahya and Saghir [39]	Al_2O_3 based nanofluids	Flat Tube	12% Heat transfer escalation at 2 vol. % of nanofluids as compared to the water, whereas the enhancement was 5% at 1 vol. % concentration of nanoparticles.
Erdogan et al. [40]	Al_2O_3/EG-water	Flat Tube	They reported 9.52% increment in heat transfer rate 4 m/s velocity of air nanofluids flow rate of 10 LPM. They reported an increase in pressure drop for the nanofluids however overall performance index was reported to increase by 18.8% at 4 m/s velocity of air.
Ahmed et al. [41]	TiO_2/water	Flat Tube	47% improvement in effectiveness of radiator due to the use nanofluids.
Sundari et al. [42]	Al_2O_3/glycerin	Flat Tube	The volume concentration was varied in the range of 0.1-0.3 vol. % and an enhancement of 54.56% in heat transfer was reported along with 90% effectiveness of radiator at 0.3 vol.% and 1500 Reynolds number.
Said et al. [43]	Al_2O_3 /EG-water and TiO_2/EG-water	Flat Tube	24.21% improvement in Nu performance of radiator as compared to the base fluid when 0.3 vol/% of nanoparticles was dispersed in base fluid. Alumina based nanofluids outperformed the titanium based nanofluids.

Reference	NF	Tube Geometry	Major Findings
Jadar et al. [44]	*f*-MWCNT/water	Flat Tube	Observed 45% enhancement in heat transfer rate as compared to the base fluid.
Bejjam et al. [45]	Al_2O_3 NFs	Flat Tube	Utmost increment of 10.64% in Nu 3.82% in heat transfer coefficient.
Selvam et al. [62]	Graphene/EG-water	Flat Tube	A range of 0.1-0.5 vole l.% concentration, 10 g/s – 100 g/s flow rate of nanofluid, and inlet temperature of 35 ℃ and 45 ℃ was tested. They reported 20% enhancement in CHTC for 0.5 vole %, 100 g/s and 35 ℃ inlet temperature. An increment of 51% in CHTC at 0.5 vol.%, 100 g/s and 45 ℃ inlet temperature was reported.
Goudarzi and Jamali [63]	Al_2O_3 /EG	Flat Tube with Wire Coil Inserts	An increment of 5% in thermal performance for nanofluid based system of coil inserts was reported.
Rai et al. [64]	MgO/EG-water	Flat Tube	Flow rate and nanoparticle concentration augmentation was concluded to be the major cause of heat transfer performance intensification. Percentage of heat transfer augmentation increases from 5.59% to 29.83% when the nanoparticle concentration increases from 0.1 vol.% to 0.2 vol.%.
Li et al. [65]	SiC-MWCNT/EG	Flat Tube	Topmost augmentation in heat transfer coefficient was 26% at 0.4 vol.% concentration.
Choi et al. [66]	Al_2O_3 /EG-water	Round Tube	6.9% increase in heat transfer rate was reported.
Kahani et al. [67]	CuO/EG-water	Shell and Tube	Reynolds number increment increased the thermal performance of the nanofluid based system.
Soylu et al. [68]	Cu and Ag dopped TiO_2/EG-water	Flat Tube	Maximum increment in CHTC was reported to be 26.15% for 1 vol.% concentration and an increment of 27.72% was reported at 2 vol.% concentration of NF.
Safikhani et al. [69]	Al_2O_3/water	Flat Tube	Increase in heat transfer was reported.
Safikhani et al. [70]	Al_2O_3/water	Flat Tubes with Multiple Tapes	heat transfer and friction factor increased by 50% and 220% respectively.

Reference	NF	Tube Geometry	Major Findings
Ramalingam et al. [71]	Al_2O_3-SiC/EG-water	Flat Tube	Maximum increase of 28.34% in overall thermal performance was observed at 0.8 vol.% of NPs in the base fluid.
Guo et al. [72]	Al_2O_3 /water	Flat Tube	Topmost augmentation in heat transfer was reported to be 11.1%. Average pressure-drop at maximum tested NP concentration of 0.5 vol. % increased by 4.4%.
Sharma et al. [73]	CuO/water	Flat Tube	An increase of 6.75% in Nu and 14% in heat transfer coefficient was reported at 50 ℃ temperature and 9000 Reynolds number.
Alirezaie et al. [74]	MgO/water Ag/water MWCNT/water DWCNT/water	Flat Tube	Topmost increment in heat transfer was reported to be 50% and the efficiency range was 10-40%. MWCNT based nanofluid outperformed rest of the nanofluids.
Sun and Liu [75]	CuO/water and Al_2O_3/water	CPU Radiator	Nanofluid concentration range was 0.1-0.5 vol.% and the Reynolds number range was 400-2000. Convective eat transfer coefficient of Cuo/water based nanofluid was 1.1-2 times higher than the base fluid.
Oliveira et al. [76]	MWCNT/water	Flat Tube	They reported 5% decrease in heat transfer rate.
Kumar et al. [77]	Al_2O_3 /water ZnO/water CuO/water	Flat Tube	Greatest increment in heat transfer coefficient was reported to be 42.5%, 47.4%, and 51.1% for 2 vol.% Al_2O_3 /water, ZnO/water, and Cuo/water nanofluids, respectively.
Zhao et al. [78]	Al_2O_3 /water	Flat Tube	Convective heat transfer for nanofluid increased by 1.236 times as compared to the base fluid.
Abdolbaqi et al. [79]	TiO_2/Bio glycol-water	Flat Tube	Temperature ranged 30-70℃, concentration ranged 0.5-2 vol. %. Nu at 2 vol. % was 3% lesser than the base fluid. Nu increment approached 28.2% at optimum operational conditions.

Reference	NF	Tube Geometry	Major Findings
Kaska et al. [80]	AlN-Al_2O_3/water	Flat Tube	Maximum Nu values were achieved at 3 vol.% and the enhancement was about 50% as compared to the base fluid. However, the Nu enhancement was observed to dropped at 4 vol.% of nanoparticles. Moreover, heat transfer increased from 28% to 58% when the nanoparticle volume concentration increased from 1 vol.% to 3 vol.%. Whereas, at 4 vol.% concentration the heat transfer enhancement reduced to 33%.
Subhedar et al. [80]	Al_2O_3/EG-water	Flat Plate	Operation conditions were opted to be 0.2-0.8 vol.% concentration, 4-9 LPM flow rate, and 65-85 ℃ inlet temperature. At 0.2 vol. % concentration of NPs the heat transfer increased by 30%. At 0.8 vol. % concentration the Nu enhanced by 28.47% as compared to the base fluid.
Hussein et al. [81]	TiO_2/water	Flat Plate	1-4 vol. % concentration, 10,000-100,000 Reynolds number, 60-90 ℃ inlet temperature was tested. Nanoparticle Even at low concentration the efficiency improved by 20%.
Zhang et al. [82]	TiO_2/water	Flat Plate	Nu decreased with increasing nanoparticle concentration. However, the values were greater than the base fluid.
Elsaid [83]	Co_3O_4/EG-water Al_2O_3/EG-water	Flat Plate	Cobalt oxide based nanofluid outperformed aluminum oxide nanofluid in terms of thermal performance.
Tijani and Sudirman [84]	Al_2O_3/EG-water CuO/EG-water	Flat Plate	The values of observed Nus were 164.29, 193.19, and 208.71 for base fluid, 0.3 vol.% of Al_2O_3 nanofluids and 0.3 vol.% of Cuo nanoparticles, respectively.
Huminic and Huminic [85]	MWCNT-Fe_3O_4/water	Flat Plate	A decrease of 26.483% in entropy generation was observed for hybrid nanofluid as compared to the base fluid.
Ali et al. [3]	MgO/Water	Flat Plate	31% maximum increase in heat transfer was reported at 0.12 vol.%

Reference	NF	Tube Geometry	Major Findings
Ahmed et al. [86]	TiO_2/water	Flat Plate	Effectiveness increased by 47%
Chen and Jia [87]	TiO_2/EG-water	Flat Plate	10% enhancement in convective heat transfer occurred.

Summary of recent studies on application of nano fluid in helical tube heat exchanger is presented in Table 2.3.

Table 2.3. Summary of recent studies on application of nano fluid in helical tube heat exchanger.

Reference	NF	Tube Geometry	Major Findings
Huminic and Huminic [50]	TiO_2/water CuO/water	Counter flow double pipe helical tube	They observed 14% greater rate of heat transfer for 2 vol.% Cuo/water nanofluid flowing at same flow rate through inner tube and the annulus
Bahremand et al. [51]	Ag/water	Helically coiled tube	They observed greater heat transfer as well as higher pressure drop in the helical tubes.
Kumar et al. [52]	MWCNT/water	Counter flow double pipe helical tube	They reported 30% enhancement in Nu for 0.6 vol.% of nanofluid at 1400 Dean number. Moreover, at 2200 Dean number, the pressure drop reached up to 11% as compared to the base fluid.
Radkar et al. [53]	ZnO/water	Helically coiled tube	They obtained 18.6% enhancement in Nu for 0.25 vol. % concentration of nanoparticles in the base fluid.
Singh et al. [54]	CNT/water	Helically coiled tube	Elevation in overall heat transfer coefficient of 62.62% as compared to the base fluid was reported.
Kulkarni et al. [55]	Ag/water	Helically coiled tube	They reported 32% elevation in heat transfer coefficient as compared to the base fluid. Nu increased with increase in Dean number.
Niwalkar et al. [56]	SiO_2/water	Helically coiled tube	Presence of nanofluid increased the heat transfer coefficient by 28.71%.
Bhanvase et al. [57]	Polyaniline (PANI)/water	Helically coiled tube	Heat transfer coefficient was obtained to be 10.52% higher than the base fluid at 0.1 vol.% loading of nanoparticles. Whereas the enhancement reached up to 69.62% at 0.5 vol.% concentration of nanoparticles in the base fluid.

Reference	NF	Tube Geometry	Major Findings
Bahiraei et al. [58]	Al_2O_3/water	Helically coiled tube	They observed increment in heat transfer as well as pressure drop.
Narrein and Mohammed [59]	Al_2O_3, SiO_2, Cuo, and ZnO based NF	Helically coiled tube	Convective heat transfer was reported to deteriorate past 2 vol.% concentration due to anomalous pressure drop that diminishes the overall effectiveness of nanofluids in helical tubes.

A review of the literature reveals that the shape of the heat exchanger tubes has a significant impact on the performance of nanofluid. Moreover, the presence of nanofluid raises the performance of heat exchanger as well. There are very limited studies on analyzing nanofluids in helical-coiled tubes with nanofluids [89].

PART 3

MATERIAL AND METHOD

Because of the importance of the thermal performance of heat exchangers and the development of techniques known as heat transfer enhancement techniques, where these technologies increase heat transfer by convection by reducing the thermal resistance in the heat exchanger.

The use of large technologies leads to an increase in heat transfer and because at the expense of the decrease in pressure and to reach a high heat transfer rate with an increased pumping capacity, different technologies are presented at the present time. One of these techniques is coiled tube technology and coiled conical tube technology as modern techniques. These tubes have been widely used in various industries because of their good performance, low cost, and ease of manufacture.

3.1. IMPORTANT DEFINITIONS

Nusselt number defined as [90]

$$Nu = \frac{hD}{k} \tag{3.1}$$

Where h (W/m^2K) is the convective heat transfer coefficient, d (m) is the pipe diameter, and k (W/mK) is the thermal conductivity.

Darcy friction factor is defined as [90]:

$$f = \frac{\Delta P}{(\rho V^2/2)(L/d)} \tag{3.2}$$

Where ΔP the pressure drop is across the test section and ρ is the density in the fluid and v^2 is the square value of the fluid velocity and L is the length of the tube d is the tube diameter.

Reynolds number is defined as [90]:

$$Re = \frac{\rho dV}{\mu} \tag{3.3}$$

Where μ (Ns/m^2) is the dynamic viscosity of the fluid.

Performance Evulation Criteria (*PEC*) is defined as [90]:

$$PEC = \frac{\frac{h_{nf}}{h_{bf}}}{\sqrt[3]{\frac{\Delta P_{nf}}{\Delta P_{bf}}}} \tag{3.4}$$

Where h_{nf} (W/m^2K) is the convective heat is transfer coefficient of nanofluid and h_{bf} (W/m^2K) is the convective heat transfer coefficient of base fluid, ΔP_{nf} is the pressure drop (Pa) of nanofluid and ΔP_{bf} (Pa) is the deferent pressure of base fluid.

3.2. CALCULATE THE TERMOPHYSICAL PROPERTIES OF NANOFLUIDS

Nanoparticles can be produced in many geometric shapes. It was observed that the change in the shape of the nanoparticles affects the thermal conductivity of the nanofluid as well as its size. In the current study three different shapes of Al_2O_3 nanoparticles (platelet, blade and cylindrical) with three different sizes (1.0%, 2.0% and 3.0%) were used. An overview of the nanoparticle shapes in Fig 3.1 and thermo-physical properties at 300 *K* in Table 3.2 [96].

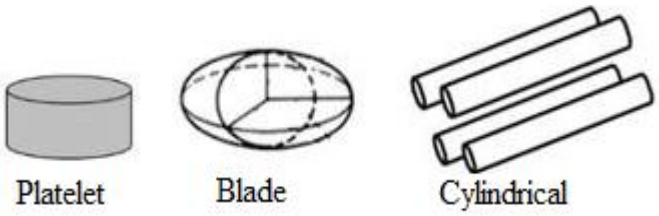

Figure 3.1. General view of commonly used nanoparticle types [66].

Table 3.1. Thermophysical properties of nanoparticle and base fluid [66].

Thermo physical Properties	***Pure Water***	***Al_2O_3***
ρ (kg/m^3)	997	3970
μ (Ns/m^2)	0.000855	-
k (W/mK)	0.613	40
c_p (J/kgK)	4179	765

The density ρ (kg/m^3) of a nanofluid can be calculated using the classical mixture theory using the following equation [66]

$$(\rho)_{nf} = (1-\varphi)\rho f + \varphi p_p \tag{3.5}$$

Where, ρ_p (kg/m^3) is density of the nanoparticle, ρ_f (kg/m^3) is density of the base fluid and $(\rho)_{nf}$ (kg/m^3) is the density of the nanofluid.

Heat capacity c_p (*J/kgK*) of the nanofluid can be calculated using the following equation [66]:

$$(c_p)nf = \left[(1-\varphi)\rho f(c_p)f + \varphi\rho_p(c_p)_p\right]/(\rho)_{nf} \tag{3.6}$$

The thermal conductivity *k* (*W/mK*) coefficient was calculated using the constants for different nanoparticle shapes that take different values depending on the shape. These values are the thermal conductivity coefficient according to the nanoparticle type as shown in Table 32, and thermal conductivity is calculated with Eq. (3.7) [96].

Table 3.2. Surface resistance and shape effects of Al_2O_3 nanoparticle [66].

	Platelet	Cylindrical	Blade
Aspect ratio	1:1/8	1:8	1:6:1/12
Sphericity, Ψ	0.52	0.62	0.36
Shape factor, n=3/Ψ	5.7	4.9	8.6
c_k	2.61	3.95	2.74
$(c_k)^{shape}$	5.72	4.82	8.26
$(c_k)^{surface}=c_k-(c_k)^{shape}$	-3.11	-0.87	-5.52

$$k_{nf} = \left[1 + [c_k \cdot \varphi]\right]k_f \tag{3.7}$$

where, $(c_k)^{surface}$ is the coefficient of thermal conductivity and is taken from Table 3.3 according to the nanoparticle type. k_f is the thermal conductivity for base fluid [66].

The dynamic viscosity μ (Ns/m^2) of the nanofluid is obtained from Eq. (3.8) where A_1 and A_2 are constants are presented in Table 3.4 [98].

Table 3.3. Viscosity coefficient for different nanoparticle shapes [66].

Nanoparticle shape	A_1	A_2
Blade	14.6	123.3
Cylindrical	13.5	904.4
Platelet	37.1	612.6

$$\mu_{nf} = \mu_f(1 + A_1\varphi + A_2\varphi^2) \tag{3.8}$$

In order to make the calculations, firstly, the velocity (*m/s*) at the specific Reynolds number has been calculated using the following equation.

$$V = (Re\mu)/(\rho D) \tag{3.9}$$

After calculations the outlet temperature (T_o), the wall temperature (T_w), and pressure drop into the tube (ΔP) have been determined. The bulk temperature T_b has been calculated using the following equation [96].

$$T_b = (T_{i+}T_o)/2 \tag{3.10}$$

In order to calculate the convective heat transfer coefficient (W/m^2K), sequential equations need to be solved [66]:

$$h = q''/(T_{w-}T_b) \tag{3.11}$$

The physical properties of the nanofluids have been calculated at the bulk temperature.

3.3. NUMERICAL SIMULATION

ANSYS Fluent software is a simulation software and used in engineering. The software is generally used after the product design and prototype stage it allows testing to be conducted in a virtual environment prior to production. of parts and parts With the help of *2D* and *3D* simulation of product assembly, strength, To improve the design by examining aspects such as mechanical and vibration. Helps [99].

ANSYS Fluent is a *CFD* software that uses the finite volume method. It has been used in many industries around the world since 1983. It evolves into the most widely used software in the *CFD* market worldwide. *ANSYS* Fluent is the most advanced Commercial *CFD* software. Quick and easy solutions to the most difficult user problems displays [99].

ANSYS Fluent, as a general purpose *CFD* software, is used in the automotive and aviation industries Industry, white goods industry, turbine machinery (fans, compressors, pumps, turbines etc.) industry, chemical industry, food industry. In solving problems of fluid mechanics and heat transfer in many industries using this.

Thanks to this feature, many different it provides an opportunity to solve the problem using the same interface. Acnes fluent, halal Thanks to its technology and the various physical models it contains, Transitional and turbulent flows, including conduction, convection, radiation, and heat transfer. Problems involving chemical reactions, fuel cells, acoustics and flow Research and development by producing solutions to problems involving noise and multiphase flows. It is a candidate to be the most reliable tool for partitions during design. The process of computational analysis, engineering modeling, and digital networks, analysis and consists of processing the results. Modeling of digital processes and networks stages of creation. Expected accuracy in the results obtained the level corresponds to a significant increase in these requirements. Liquids this is in the analysis of mechanics and heat transfer problems by numerical methods Maintain requirements within reasonable limits and achieve usable results. In order to be able to do this, a multi-stage path is followed from simple to complex [99].

In this study, the outlet temperature of the nanofluid and the tube wall temperature have been determined to calculate the average Nusselt number. Pressure drop have been determined on the inlet and outlet section for calculate average Darcy friction factor. The aim of the study is to numerically analyze the changes in velocity, temperature and pressure with the change in Reynolds number. Numerical analysis was simulated in the *ANSYS* Fluent software.

The *ANSYS* Fluent software is divided into five main steps to reach the desired result;

- Create geometry (Geometry)
- Create a mesh (Mesh)
- Defining the problem and boundary conditions (Setup)
- Analysis (Solution)
- Analyze the results (Results).

3.3.1. Creating Geometry

In the first step of the study, coiled conical tube was drawn in *2D* in AutoCAD software and then introduced to *ANSYS* Fluent program. The appearance and size of the coiled conical tube are shown in (Fig 3.2). Also the diameters are given in Table 3.1.

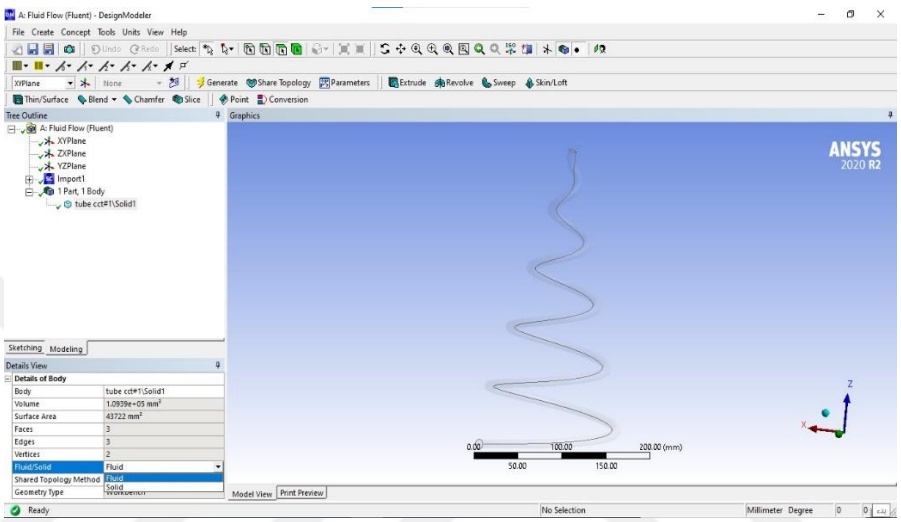

Figure 3.2. Schematic diagram of conical coil tube.

Table 3.4. Coiled conical tube dimensions.

Inner diameter d (mm)	Thickness of pip T(mm)	Length of pip L (mm)	Pitch circle diameter D (mm)	Helical pitch b (mm)	Cone angle α (deg)	Height H (mm)
10	0.8	1500	170	65	30	317.22

3.3.2. Creating Mesh

Mesh structure is the most important part for *CFD* analysis. The error to be made at this stage will directly affect the solving time of the software and the results to be obtained as a result of the solution. As the number of cells increases, the solution time will also increase. Therefore, mesh optimization should be analyzed and the optimum mesh number should be determined. In addition, by ensuring that regions of less importance during analysis have lower mesh counts, we can keep our total mesh

count lower and reduce our resolution time. The cross-sectional view of the coiled conical tube and the mesh structure are given in Fig 3.3. Some areas have been meshed more frequently to ensure that the results are more precise.

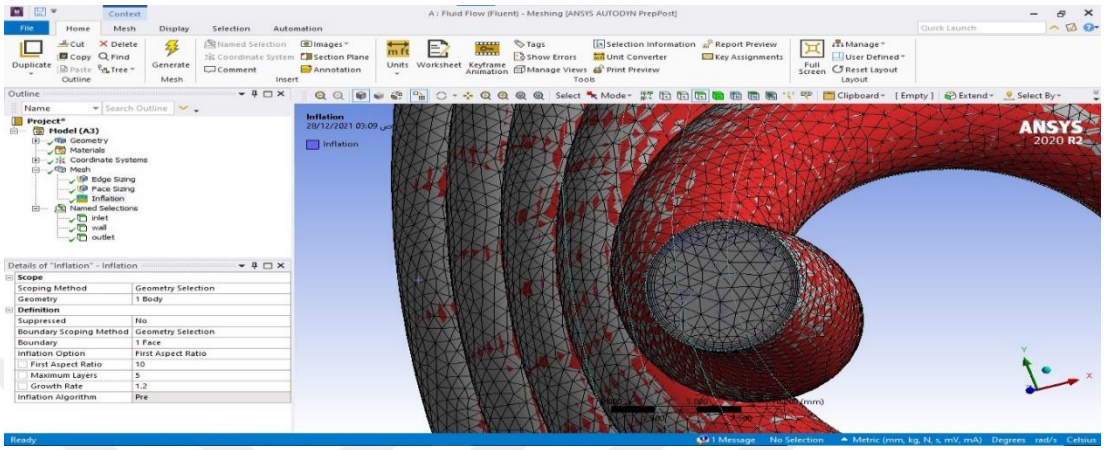

Figure 3.3. Cross-sectional view of the coiled conical tube and the mesh structure.

3.3.3. Defining the Problem and Boundary Conditions

At this stage of the numerical study, boundary conditions and fluid properties are manually defined to the system and introduced into the program. Screenshot taken from the ANSYS software was shown in Fig 3.4.

The studies have been primarily carried out with distilled water and confirmed by the literature. Then, Al_2O_3 nanofluid has been used as the working fluid. Thermophysical properties of the nanofluid for each nanoparticle volumetric ratio and nanoparticle shape have been calculated using the relations and introduced to the software before the numerical study.

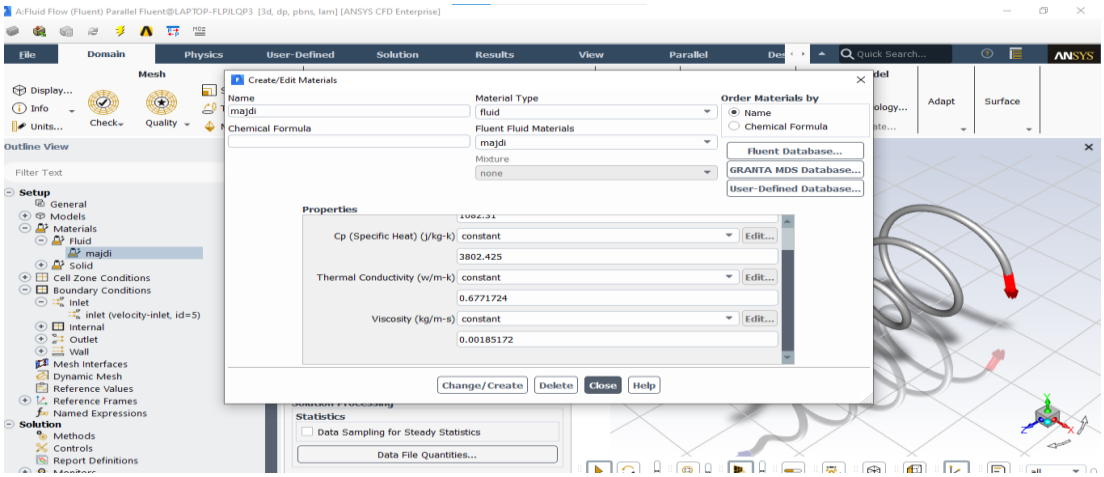

Figure 3.4. Thermophysical properties of the working fluid.

3.3.4. Analysis

In the solution phase, the desired iteration number or value is selected over the software. Then, initilation process was performed and analysis was started. In our study, iterations continued until the values approached $1x10^{-6}$. An example screenshot is given in Fig 3.6.

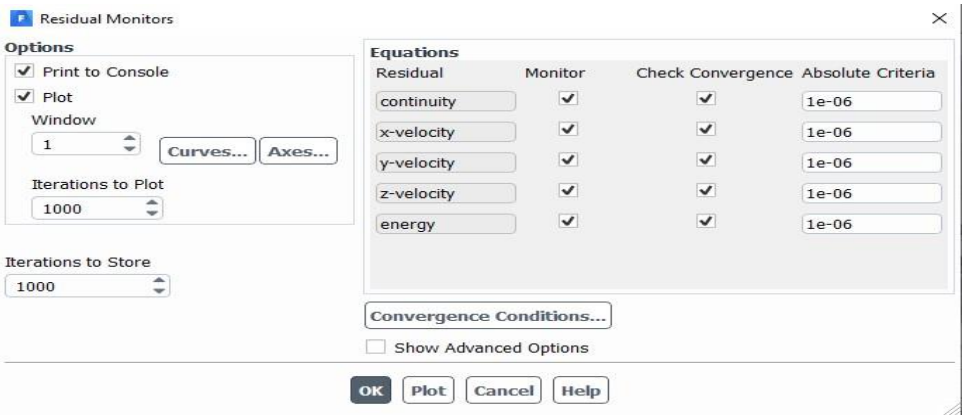

Figure 3.5. Residuals monitors.

3.3.5. Analyze the Results

After the completion of the numerical work, contour graphics, vectors and animations have been examined and the results were reviewed.

PART 4

RESULTS AND DISCUSSIONS

4.1. MESH OPTIMIZATION AND VALIDATION OF THE NUMERICAL CODE

On the basis of numerical analysis, it must be proven that the number of meshes assigned for the solution does not affect the results obtained. Nusselt number and Darcy friction factor values were obtained by performing analyzes in different mesh numbers for the highest Reynolds number (*Re=2150*) value of the boundary conditions determined to prove this. The obtained results are shown in Table 4.1.The error percentages for each variable are found in the table, and it is noticed that the change in Nusselt number and Darcy friction factor values is very small especially after $1.4x10^6$ mesh number. Accordingly, the optimum number of meshes is found to be $1.4x10^6$ for faster and more accurate results.

Table 4.1. Variation of *Nu* and *f* with mesh number.

No	Edge Sizing (Number of Division)	Face Sizing (Element Size)	Mesh Number (Element Number)	Changing Mesh Number (Element Number)%	Nusselt Number *Nu*	Changing *Nu*%	Darcy Friction Factor *f*	Changing *f* (%)
1	20	4	45585	-	26.757	-	0.10992	-
2	25	3.5	57859	26.92	25.312	-5.70	0.09455	-16.25
3	30	3	81753	41.29	25.677	1.42	0.09017	-4.8
4	35	2.5	$1.303*10^5$	59.43	25.569	-0.42	0.08495	-6.1
5	40	2	$1.9818*10^5$	52.04	25.671	0.39	0.08500	0.05
6	45	1.5	$3.851*10^5$	94.32	25.843	0.66	0.08641	1.63
7	50	1	$1.35*10^6$	168.7	25.507	-1.30	0.08629	-0.14
8	55	0.8	$1.04*10^6$	0.63	25.56	0.21	0.08645	0.18
9	60	0.7	$1.7*10^6$	68.49	25.08	-1.92	0.08512	-1.5
10	65	0.6	$2.4*10^6$	38.67	24.82	-1.02	0.08471	-0.4
11	60	0.5	3.610^6	49.69	24.61	-0.86	0.08476	0.05
12	65	0.5	$5.5*10^6$	51.07	24.46	-0.61	0.08568	1.06

Studies have been performed for different Reynolds numbers and obtained mean Nusselt number with using the solution area with the optimum mesh number obtained. These results were compared with those of Heyhat et al. [61] and the accuracy of the numerical study has been tested. Then, using the proven coiled conical tube geometry and mesh optimization, nanofluids were used into the system and analyzes have been started. The average difference between the experimental and numerical results was ∓8% as showing in Table 4.2. The variation of average Nusselt numbers for numerical results and experimental data are given in Fig 4.1.

Table 4.2. Comparison of the results of numerical analysis with literature (pure water).

No	Reynolds Number	Experimental Results	Numerical Results	Error value %
1	1000	15.36	14.88	3.125
2	1250	17.05	17.45	-2.346
3	1500	19.02	19.84	-4.311
4	1750	20.87	22.11	-5.941
5	2000	22.61	24.26	-7.297
6	2150	23.61	25.51	-8.047

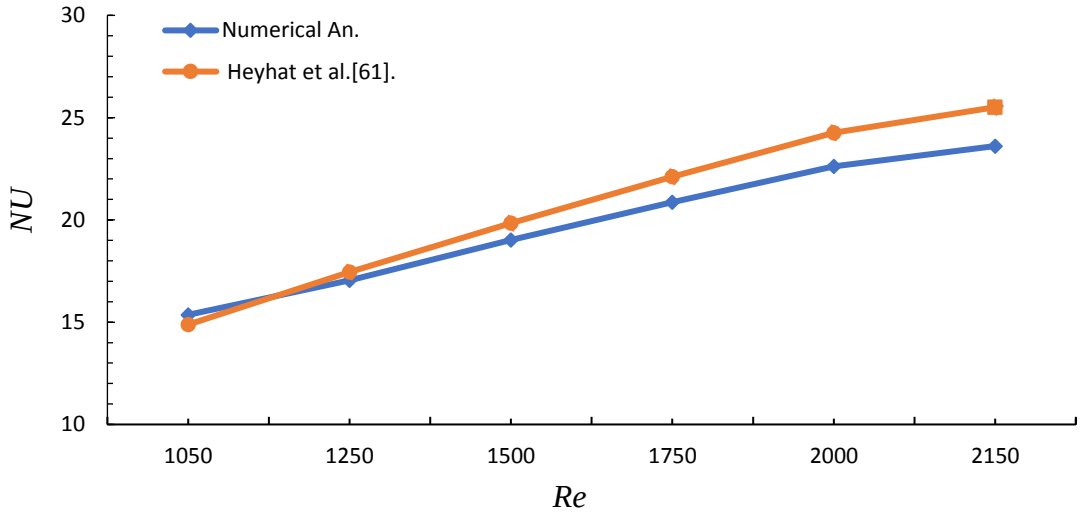

Figure 4.1. Comparison of numerical results with literature.

4.2. EFFECT OF CHANGING NANOPARTICLE ON AVERAGE NUSSELT NUMBER

All results are collected in excel workbook. Equations were defined for the necessary calculations and graphs were drawn based on the relevant parameters.

4.3.1. Effect the Nanoparticles Volume Ratio on Average Nusselt Number

Platelet Nanoparticles:

The effect of the change of platelet nanoparticle volume fraction on the average Nusselt number is analyzed for 1.0%, 2.0% and 3.0% in Fig 4.2. Compared with pure water, 20.3%, 26.0% and 31.0% higher Nusselt number were obtained with %1.0, %2.0 and %3.0 nanoparticle volume ratio, respectively.

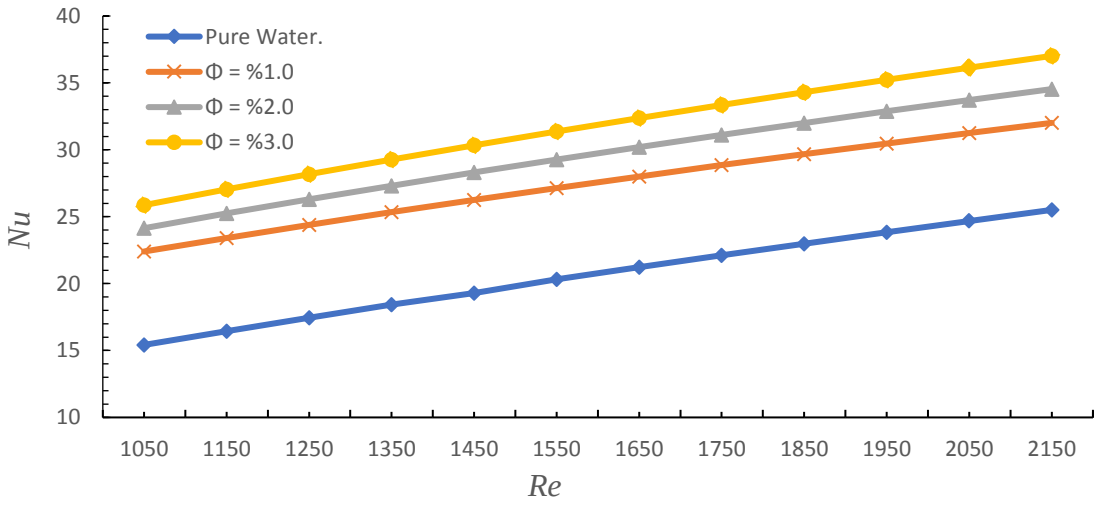

Figure 4.2. Effect of the platelet nanoparticle volume ratio on average Nusselt number.

Blade Nanoparticles:

The effect of the change of blade nanoparticle volume fraction on the average Nusselt number is analyzed for 1.0%, 2.0% and 3.0% in Fig. 4.3. Compared with pure water, 15.6%, 17.5% and 19.5% higher Nusselt number were obtained with %1.0, %2.0 and %3.0 nanoparticle volume ratio, respectively.

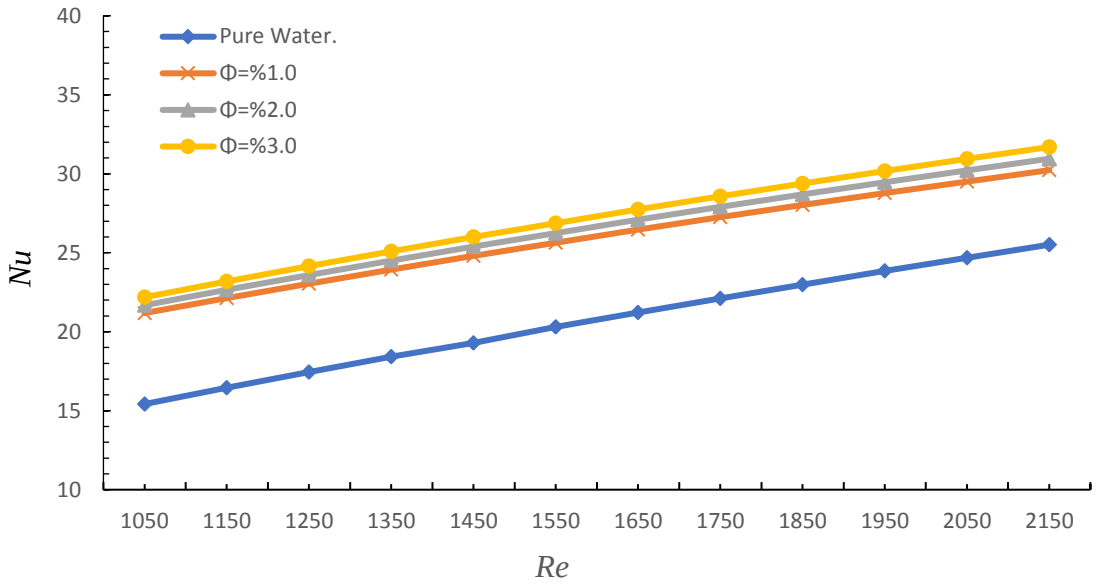

Figure 4.3. Effect of the blade shape nanoparticle volume ratio on average Nusselt number.

Cylindrical Nanoparticles:

The effect of the change of cylindrical nanoparticle volume fraction on the average Nusselt number is analyzed for 1.0%, 2.0% and 3.0% in Fig 4.4. Compared with pure water, 16.3%, 21.2% and 28.6% higher Nusselt number were obtained with %1.0, %2.0 and %3.0 nanoparticle volume ratio, respectively.

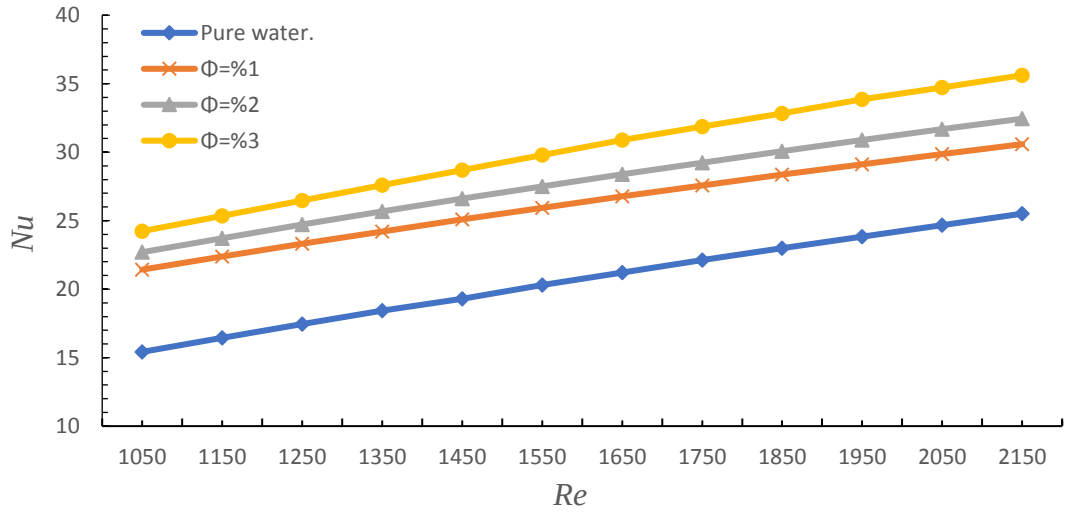

Figure 4.4. Effect of the cylindrical shape nanoparticle volume ratio on average Nusselt number.

As can be seen from Fig.4.2, 4.3 and 4.4, 3.0% *NPVC* provided the highest heat transfer rate in all nanoparticle shapes. According to the results obtained by changing the nanoparticle shape, it was observed that the highest heat transfer rate was achieved in the form of platelet nanoparticles

4.2.2. Effect of Nanoparticle Shape on Average Nusselt Number

Effect of the nanoparticle shape at 1.0% volume ratio on average Nusselt number:

The effect of changing nanoparticle shapes on average Nusselt number is numerically analyzed for 1.0% nanoparticle volume ratio in Fig 4.5.

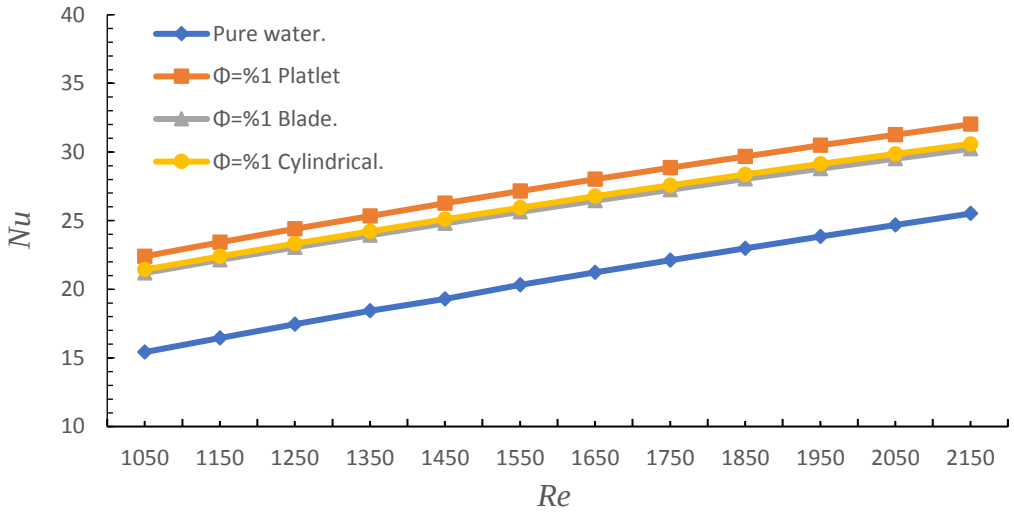

Figure 4.5. Effect of the nanoparticle shape at 1.0% nanoparticle volume ratio on the average Nusselt number.

Effect of the nanoparticle shape at 2.0% volume ratio on average Nusselt number:

The effect of changing nanoparticle shape on average Nusselt number is numerically analyzed for 2.0% nanoparticle volume ratio in Fig 4.6.

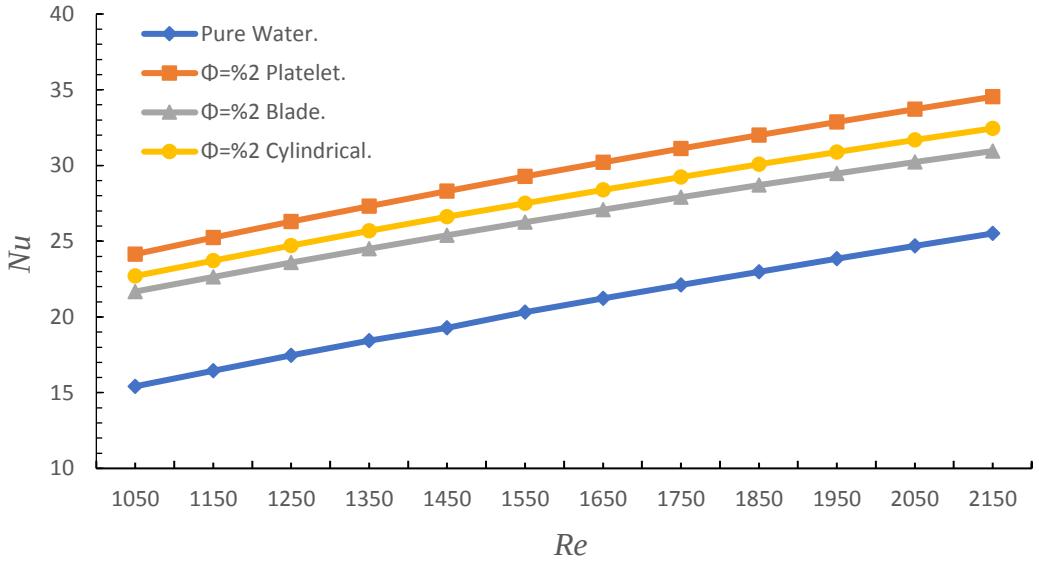

Figure 4.6. Effect of the nanoparticle shape at 2.0% nanoparticle volume ratio on the average Nusselt number.

Effect of the nanoparticle shape at 3.0% volume ratio on average Nusselt number:

The effect of changing nanoparticle shapes on average Nusselt number is analyzed for 3.0% nanoparticle volume ratio in Fig 4.7.

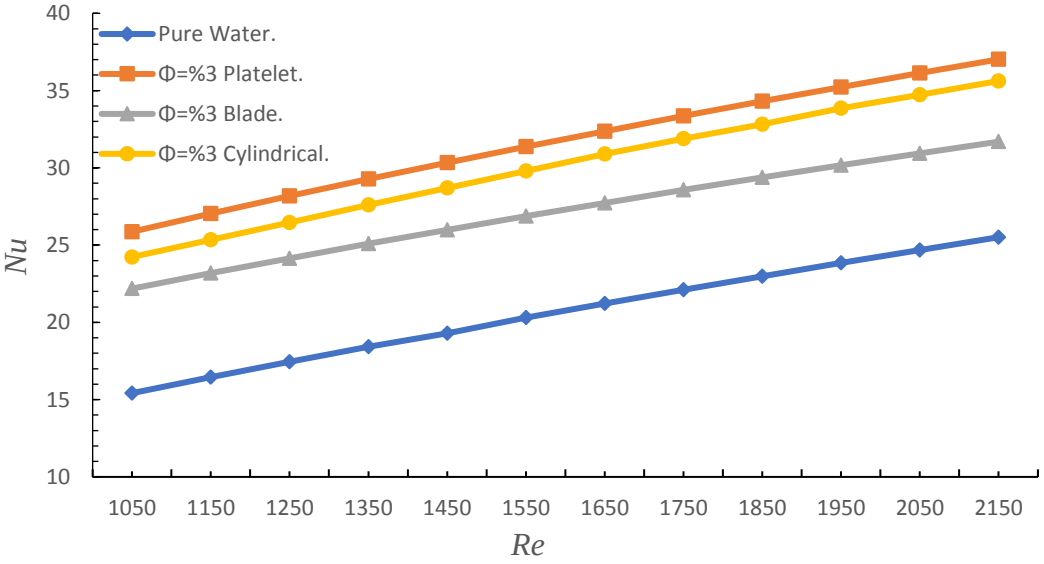

Figure 4.7. Effect of the change of nanoparticle shape at 3.0% nanoparticle volume ratio on the average Nusselt number.

Temperature distribution for Al2O3-water nanofluid with platelet nanoparticle with platelet nanoparticle in the tube and at the outlet section are given in the Fig 4.8 and Fig 4.9, respectively.

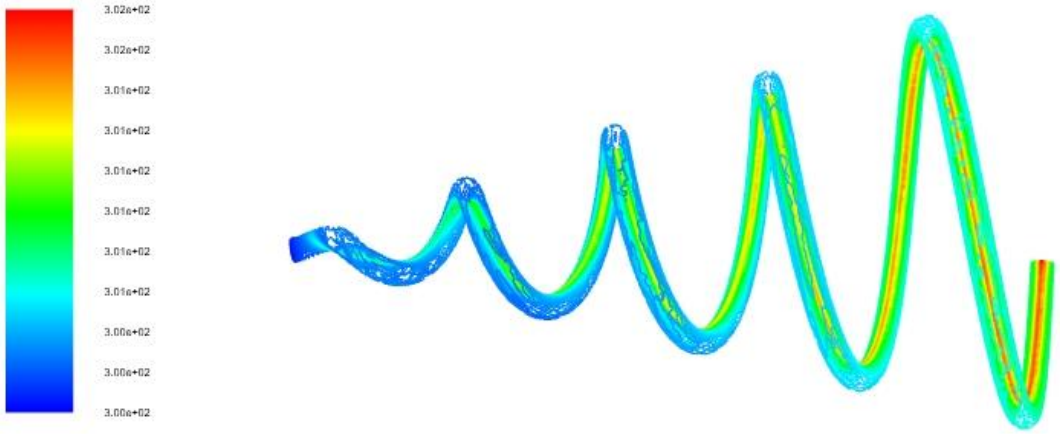

Figure 4.8. Temperature distribution of 3.0% nanoparticle volume ratio of Al_2O_3-water nanofluid with platelet nanoparticle in the tube.

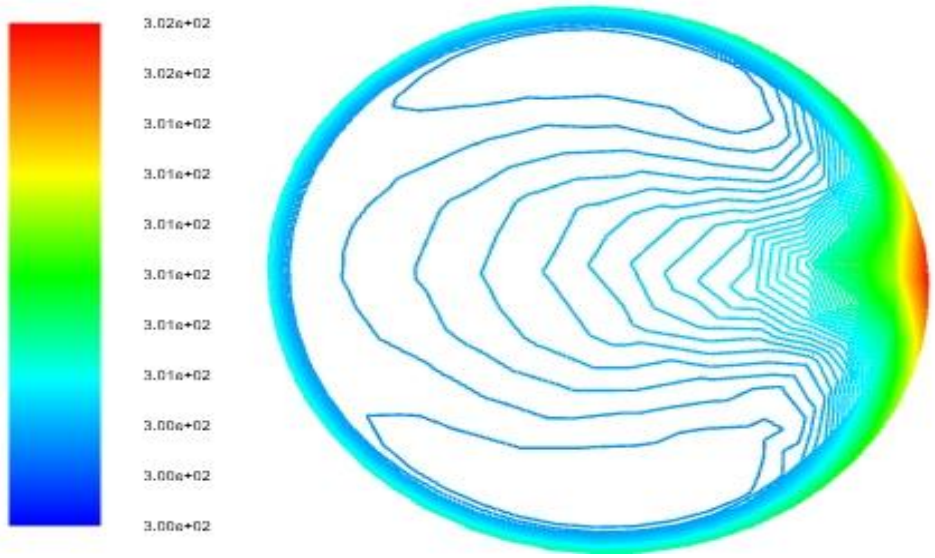

Figure 4.9. Temperature distribution of 3.0% nanoparticle volume ratio of Al_2O_3-water nanofluid with platelet nanoparticle at the outlet section.

4.3. THE EFFECT OF THE CHANGE OF NANOPARTICLE VOLUME RATIO ON THE AVERAGE DARCY FRICTION FACTOR

It was found that the change of nanoparticle shape and volumetric ratio did not change the average Darcy friction factor as showing in the Fig 4.10, (Fig 4.11, and Fig 4.12, respectively.

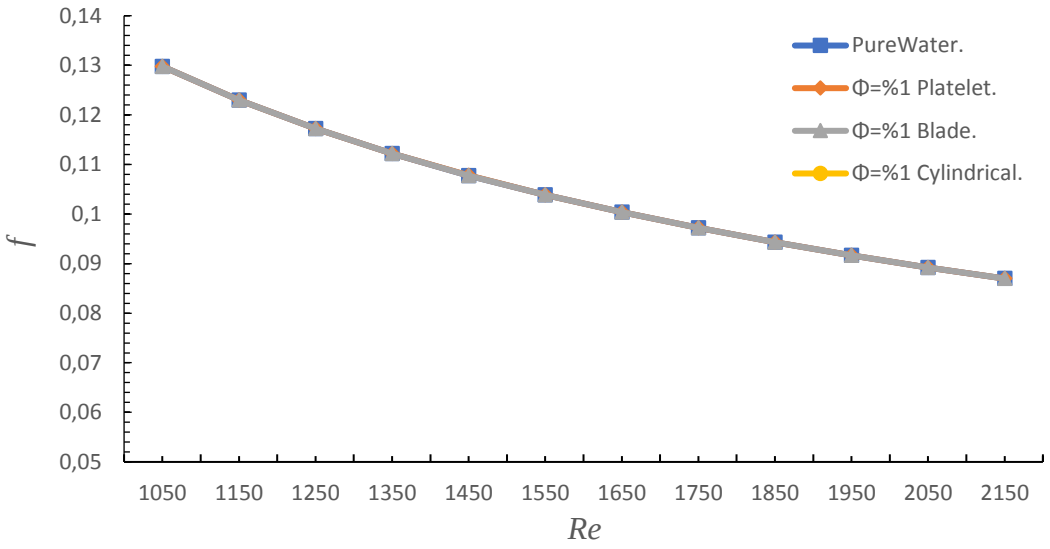

Figure 4.10. . Effect of the nanoparticle shape at 1.0% nanoparticle volume ratio on the average Darcy friction factor.

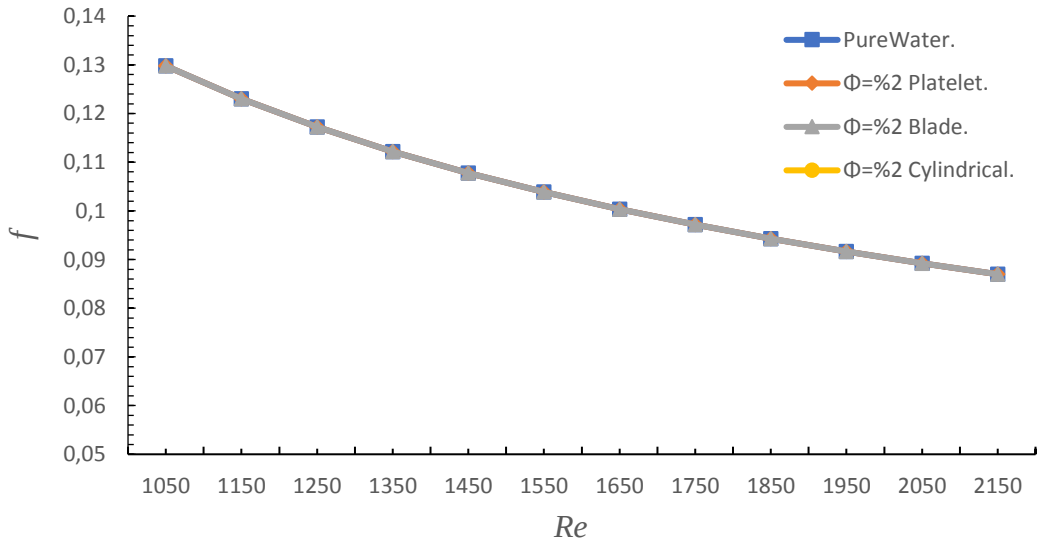

Figure 4.11. Effect of the nanoparticle shape at 2.0% nanoparticle volume ratio on the average Darcy friction factor.

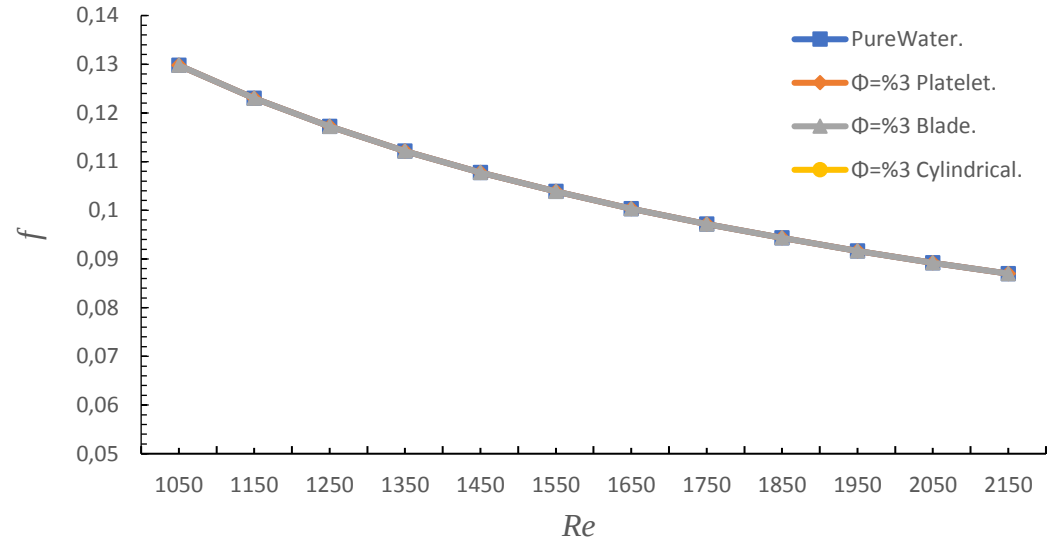

Figure 4.12. Effect of the nanoparticle shape at 3.0% nanoparticle volume ratio on the average Darcy friction factor.

4.5. PERFORMANCE EVALUATION CRITERIA

PEC value above 1 was obtained for all nanoparticle shapes. The fact that the PEC value is above 1 clearly shows that for all nanoparticle shapes, the amount of heat transfer increases more than the increase in pressure drop, and the utility model is provided. The results obtained are given in Figs 4.13, 4.14 and 4.15.

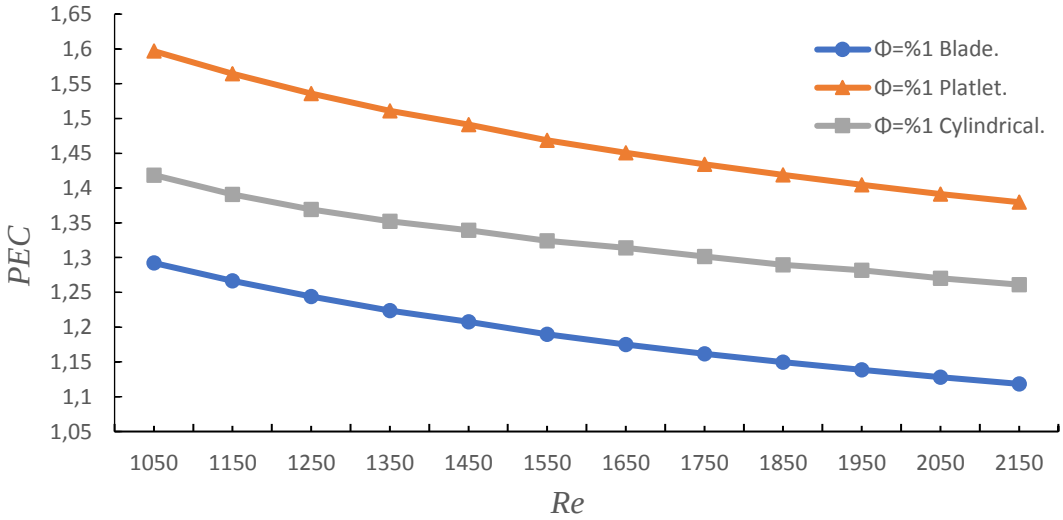

Figure 4.13. Effect of nanoparticle shape change on *PEC* number in 1.0% *NPVC*.

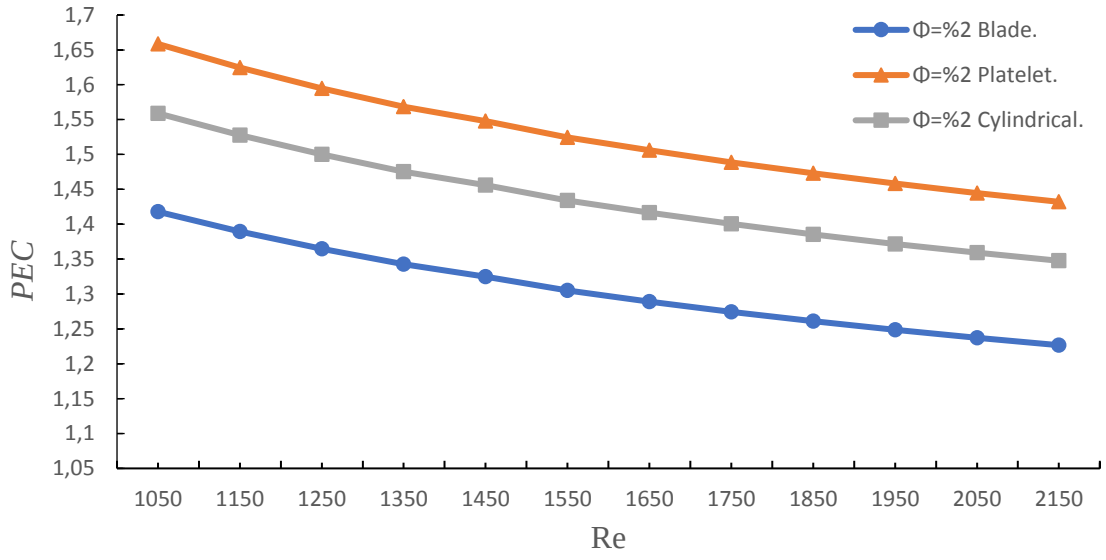

Figure 4.14. Effect of nanoparticle shape change on *PEC* number in 2.0% *NPVC*.

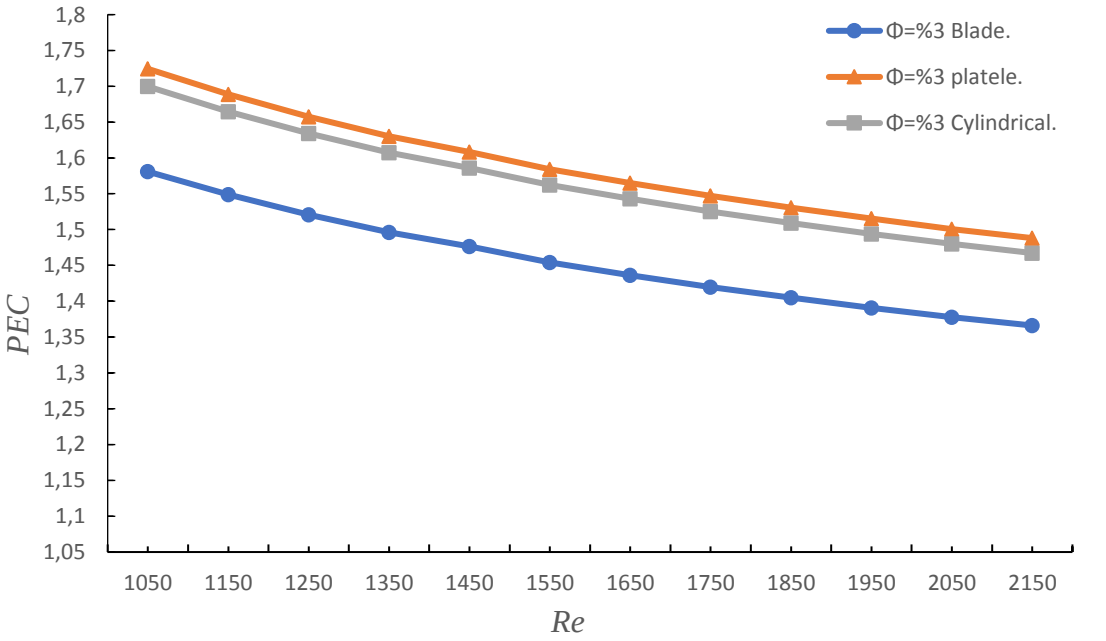

Figure 4.15. Effect of nanoparticle shape change on *PEC* number in 3.0% *NPVC*.

The *PEC* value is directly related to the pressure drop. Basically, for the PEC value to be large, we need to gain more energy as heat transfer than we lose in the pressure drop. The pressure distribution over the geometry is shown in Fig 4.16.

Figure 4.16. Pressure distribution on in the tub.

PART 5

CONCLUSION AND RECOMMENDATIONS

5.1. CONCLUSION

In this study, 1.0%, 2.0% and 3.0% *NPVC* of Alumina (Al_2O_3)-water nanofluid flow in a conical helical tube with platelet, blade and cylindrical nanoparticle shapes numerically analyzed under laminar flow ($1050 \leq Re \leq 2150$) condition. The findings of the study are summarized below:

- The value of the Reynolds number and the Nusselt number change proportionally for all nanoparticle shapes.
- The value of the Reynolds number and the Darcy friction factor number varies inversely for all nanoparticle shapes.
- The pressure drop increases when the nanoparticle volume ratio increases, and he highest pressure drop was achieved when 3.0% platelet type nanofluid was used.
- Changing the nanoparticle shape did not affect the Darcy friction factor value.
- It has been determined that the value of the NPVC and the average Nusselt number change proportionally for all nanoparticle shapes. Therefore, the highest convection heat transfer rate were obtained at 3.0% nanoparticle volume ratio for each nanoparticle shape.
- The highest convective heat transfer performance is observed with the platelet nanoparticle shape.
- The highest PEC value is obtained for platelet shaped nanoparticle with 3.0% nanoparticle volume ratio.
- Conical helical tubes are one of the good option for heat exchange devises for higher heat transfer performance with small pressure drop penalty.

5.2. RECOMMENDATIONS

Taking into account the results obtained in this study, it should be studied to improve heat transfer by forced convection by adding nanoparticles of different materials to improve heat transfer in conical helical tubes and other tubes.

After conducting this study and analyzing and listing the results, they can be summarized as follows:

- The nanoparticle volume ratio and the rate of heat transfer are directly proportional up to 3.0%. Higher values should be sought.
- It can be compared with platelet, blade and cylindrical shapes by using different nanoparticle shapes.
- Different conical helical tubes with different conical diameters can be analyzed.

REFERENCES

[1] H.M. Ali, T.R. Shah, H. Babar, Z.A. Khan, Application of NFs for Thermal Management of Photovoltaic Modules: ***A Review, in: Microfluid. NFics, InTech,*** 2018. doi:10.5772/intechopen.74967.

[2] H.M. Ali, A. Arshad, M. Jabbal, P.G. Verdin, Thermal management of electronics devices with PCMs filled pin-fin heat sinks: A comparison, Int. ***J. Heat Mass Transfer***. 117 (2018) 1199–1204. doi:10.1016/j.ijheatmasstransfer.2017.10.065.

[3] H. Ali, M. Azhar, M. Saleem, Q. Saeed, A. Saieed, HT enhancement of car radiator using aqua based magnesium oxide NFs, ***J.Therm. Sci.*** 19 (2015) 2039–2048. doi:10.2298/TSCI150526130A.

[4] X.Q. Wang, A.S. Mujumdar, HT characteristics of NFs: a review, Int. ***J. Therm. Sci.*** 46 (2007) 1–19. doi:10.1016/j.ijthermalsci.2006.06.010.

[5] H. Babar, H.M. Ali, Towards hybrid NFs: Preparation, thermophysical properties, applications, and challenges, ***J. Mol. Liq.*** 281 (2019) 598–633. doi:10.1016/j.molliq.2019.02.102.

[6] H. Babar, H.M. Ali, Towards hybrid NFs: Preparation, thermophysical properties, applications, and challenges, ***J. Mol. Liq.*** 281 (2019) 598–633. doi:10.1016/j.molliq.2019.02.102.

[7] H.M. Ali, H. Babar, T.R. Shah, M.U. Sajid, M.A. Qasim, S. Javed, Preparation techniques of TiO2 NFs and challenges: ***A review, J.Appl. Sci.*** 8 (2018) 587. doi:10.3390/app8040587.

[8] F. Abbas, H.M. Ali, M. Shaban, M.M. Janjua, T.R. Shah, M.H. Doranehgard, M. Ahmadlouydarab, F. Farukh, Towards convective HT optimization in aluminum tube automotive radiators: Potential assessment of novel Fe2O3-TiO2/water hybrid NF, ***J. Taiwan Inst. Chem. Eng.*** 000 (2021) 1–13. doi:10.1016/j.jtice.2021.02.002.

[9] J.M. Munyalo, X. Zhang, Particle size effect on thermophysical properties of NF and NF based phase change materials: ***A review, J. Mol. Liq.*** 265 (2018) 77–87. doi:10.1016/j.molliq.2018.05.129.

[10] P. Keblinski, J.A. Eastman, D.G. Cahill, NFs for thermal transport, ***J. Mater. Today.*** 8 (2005) 36–44. doi:10.1016/S1369-7021(05)70936-6.

[11] S. Chakraborty, P.K. Panigrahi, Stability of NF: ***A review, Appl. Therm. Eng***. 174 (2020). doi:10.1016/j.applthermaleng.2020.115259.

[12] R. Chein, J. Chuang, Experimental microchannel heat sink performance studies using NFs, ***Int. J. Therm. Sci.*** 46 (2007) 57–66. doi:10.1016/j.ijthermalsci.2006.03.009.

[13] S.M. Vanaki, H.A. Mohammed, A. Abdollahi, M.A. Wahid, Effect of NP shapes on the HT enhancement in a wavy channel with different phase shifts, ***J. Mol. Liq.*** 196 (2014) 32–42. doi:10.1016/j.molliq.2014.03.001.

[14] M.U. Sajid, H.M. Ali, Thermal conductivity of hybrid NFs: A critical review, Int. ***J. Heat Mass Transfer..*** 126 (2018) 211–234. doi:10.1016/j.ijheatmasstransfer.2018.05.021.

[15] S. Sarbolookzadeh Harandi, A. Karimipour, M. Afrand, M. Akbari, A. D'Orazio, An experimental study on thermal conductivity of F-MWCNTs-Fe3O4/EG hybrid NF: Effects of temperature and concentration, Int. Commun. ***Heat Mass Transfer.*** 76 (2016) 171–177. doi:10.1016/j.icheatmasstransfer.2016.05.029.

[16] E. V Timofeeva, J.L. Routbort, D. Singh, Particle shape effects on thermophysical properties of alumina NFs Particle shape effects on thermophysical properties of alumina NFs, ***J. Appl. Phys.*** 014304 (2013). doi:10.1063/1.3155999.

[17] I.M. Shahrul, A comparative review on the specific heat of nanofluids for energy perspective, Department of Mechanical Engineering, ***Faculty of Engineering, University of bkey***, http://dx.doi.org/10.1016/j.rser.2014.05.081 1364-0321/& 2014 Elsevier Ltd.

[18] R. Deepak Selvakumara , Jian Wua,b,∗ A comprehensive model for effective density of nanofluids based on particle clustering and interfacial layer formation, aSchool of Energy Science and Engineering, ***Harbin Institute of*** Technology, Harbin 150001, PR China. bkey Laboratory of Aerospace Thermo ***physics, Ministry of Industry and Information Technology,*** Harbin 150001, PR China.

[19] Ernani Favale, Arturo de Risi, Domenico Laforgia, Results of experimental investigations on the heat conductivity of nanofluids based on diathermic oil for high temperature applications, Dipartimento di Ingegneria dell'***Innovazione, Università del Salento, Via per Arnesano,***73100Lecce,Italy,doi:10.1016/j.apenergy.2011.11.026.

[20] I. Chopkar, S. Sudarshan, P.K. Das, I. Manna, Effect of particle size on thermal conductivity of NF, Metall. Mater. Trans. A Phys. ***Metall. Mater. Sci.*** 39 (2008) 1535–1542. doi:10.1007/s11661-007-9444-7.

[21] N.N. Esfahani, D. Toghraie, M. Afrand, A new correlation for predicting the thermal conductivity of ZnO–Ag (50%–50%)/water hybrid NF: An experimental study, ***Powder Technol.*** 323 (2018) 367–373. doi:10.1016/j.powtec.2017.10.025.

[22] T.R. Shah, H. Koten, H.M. Ali, Performance effecting parameters of hybrid NFs, in: Hybrid NFs Convect. ***Heat Transf., Elsevier, 2020: pp***. 179–213. doi:10.1016/B 978-0-12-819280-1.00005-7.

[23] M. Hemmat Esfe, P.M. Behbahani, A.A.A. Arani, M.R. Sarlak, Thermal conductivity enhancement of SiO2–MWCNT (85:15 %)–EG hybrid NFs : ANN designing, experimental investigation, cost performance and sensitivity analysis, ***J. Therm. Anal. Calorim.*** 128 (2017) 249–258. doi:10.1007/s10973-016-5893-9.

[24] A. Ahmadi Nadooshan, H. Eshgarf, M. Afrand, Measuring the viscosity of Fe3O4-MWCNTs/EG hybrid NF for evaluation of thermal efficiency: Newtonian and non-Newtonian behavior, ***J. Mol. Liq.*** 253 (2018) 169–177. doi:10.1016/j.molliq.2018.01.012.

[25] S.H. Rostamian, M. Biglari, S. Saedodin, M. Hemmat Esfe, An inspection of thermal conductivity of CuO-SWCNTs hybrid NF versus temperature and concentration using experimental data, ANN modeling and new correlation, ***J. Mol. Liq.*** 231 (2017) 364–369. doi:10.1016/j.molliq.2017.02.015.

[26] A. Alirezaie, S. Saedodin, M.H. Esfe, S.H. Rostamian, Investigation of rheological behavior of MWCNT (COOH-functionalized)/MgO - Engine oil hybrid NFs and modelling the results with artificial neural networks, ***J. Mol. Liq.*** 241 (2017) 173–181. doi:10.1016/j.molliq.2017.05.121.

[27] A. Zareie, M. Akbari, Hybrid NPs effects on rheological behavior of water-EG coolant under different temperatures: An experimental study, J**. *Mol. Liq.*** 230 (2017) 408–414. doi:10.1016/j.molliq.2017.01.043.

[28] M.H. Esfe, S. Esfandeh, M.K. Amiri, M. Afrand, A novel applicable experimental study on the thermal behavior of SWCNTs(60%)-MgO(40%)/EG hybrid NF by focusing on the thermal conductivity, *Powder Technol.* 342 (2019) 998–1007. doi:10.1016/j.powtec.2018.10.008.

[29] K. Motahari, M. Abdollahi Moghaddam, M. Moradian, Experimental investigation and development of new correlation for influences of temperature and concentration on dynamic viscosity of MWCNT-SiO2 (20-80)/20W50 hybrid nano-lubricant, Chinese ***J. Chem. Eng.*** 26 (2018) 152–158. doi:10.1016/j.cjche.2017.06.011.

[30] K.A. Hamid, W.H. Azmi, M.F. Nabil, R. Mamat, K. V. Sharma, Experimental investigation of thermal conductivity and dynamic viscosity on NP mixture ratios of TiO2-SiO2 NFs, Int. ***J. Heat Mass Transfer.*** 116 (2018) 1143–1152. doi:10.1016/j.ijheatmasstransfer.2017.09.087.

[31] M. Hemmat Esfe, M.H. Hajmohammad, Thermal conductivity and viscosity optimization of nanodiamond-Co3O4/EG (40:60) aqueous NF using NSGA-II coupled with RSM, ***J. Mol. Liq.*** 238 (2017) 545–552. doi:10.1016/j.molliq.2017.04.056.

[32] A.S. Dalkılıç, Ö. Açıkgöz, B.O. Küçükyıldırım, A.A. Eker, B. Lüleci, C. Jumpholkul, S. Wongwises, Experimental investigation on the viscosity characteristics of water based SiO2-graphite hybrid NFs, ***Int. Commun. Heat Mass Transf.*** 97 (2018) 30–38. doi:10.1016/j.icheatmasstransfer.2018.07.007.

[33] S. Ghasemi, A. Karimipour, Experimental investigation of the effects of temperature and mass fraction on the dynamic viscosity of CuO-paraffin NF, ***Appl. Therm. Eng.*** 128 (2018) 189–197. doi:10.1016/j.applthermaleng.2017.09.021.

[34] D. Jing, Y. Hu, M. Liu, J. Wei, L. Guo, Preparation of highly dispersed NF and CFD study of its utilization in a concentrating PV/T system, ***Sol. Energy.*** 112 (2015) 30–40. doi:10.1016/j.solener.2014.11.008.

[36] H. Babar, M. Sajid, H. Ali, Viscosity of hybrid NFs: ***A critical review, Therm. Sci.*** 23 (2019) 1713–1754. doi:10.2298/TSCI181128015B.

[37] A.S. Tijani, A. Suhail, Thermos-physical properties and HT characteristics of water / anti-freezing and Al 2 O 3 / CuO based NF as a coolant for car radiator, Int. ***J. Heat Mass Transfer.*** 118 (2018) 48–57. doi:10.1016/j.ijheatmasstransfer.2017.10.083.

[38] H. Babar, H.M. Ali, Airfoil shaped pin-fin heat sink: Potential evaluation of ferric oxide and titania NFs, Energy Convers. ***Manag.*** 202 (2019) 112194. doi:10.1016/j.enconman.2019.112194.

[39] B. Farajollahi, S.G. Etemad, M. Hojjat, HT of NFs in a shell and tube HX, Int. ***J. Heat Mass Transf.*** 53 (2010) 12–17. doi:10.1016/j.ijheatmasstransfer.2009.10.019.

[40] T.R. Shah, H.M. Ali, M.M. Janjua, On aqua-based silica (Sio2–water) nanocoolant: Convective thermal potential and experimental precision evaluation in aluminum tube radiator, ***Nanomaterials.*** 10 (2020) 1–23. doi:10.3390/nano10091736.

[41] R.S. Vajjha, D.K. Das, P.K. Namburu, International Journal of Heat and Fluid Flow Numerical study of fluid dynamic and HT performance of Al 2 O 3 and CuO NFs in the flat tubes of a radiator, ***Int. J. Heat Fluid Flow***. 31 (2010) 613–621. doi:10.1016/j.ijheatfluidflow.2010.02.016.

[42] M. Elsebay, I. Elbadawy, M.H. Shedid, M. Fatouh, Numerical resizing study of Al2O3 and CuO NFs in the flat tubes of a radiator, ***Appl. Math. Model.*** 40 (2016) 6437–6450. doi:10.1016/j.apm.2016.01.039.

[43] M. Yahya, M.Z. Saghir, Thermal analysis of flow in a porous flat tube in the presence of a NF: Numerical approach, Int. ***J. Thermofluids***. 10 (2021). doi:10.1016/j.ijft.2021.100095.

[44] B. Erdoğan, İ. Zengin, S. Mert, A. Topuz, T. Engin, The experimental study of the entropy generation and energy performance of nano-fluid flow for automotive radiators, Eng. Sci. Technol. ***an Int. J. 24*** (2021) 655–664. doi:10.1016/j.jestch.2020.10.007.

[45] S.A. Ahmed, M. Ozkaymak, A. Sözen, T. Menlik, A. Fahed, Improving car radiator performance by using TiO2-water NF, Eng. Sci. Technol. ***an Int. J. 21*** (2018) 996–1005. doi:10.1016/j.jestch.2018.07.008.

[46] K.G. Sundari, L.G. Asirvatham, S. Joseph John Marshal, S. Manova, M. Sahu, M. Jesse Aaron, HT studies using glycerin based nanocoolant for car radiator cooling applications, ***j. Mater. Today Proc.*** (2021). doi:10.1016/j.matpr.2021.06.104.

[47] Z. Said, M. El Haj Assad, A.A. Hachicha, E. Bellos, M.A. Abdelkareem, D.Z. Alazaizeh, B.A.A. Yousef, Enhancing the performance of automotive radiators using NFs, ***Renew. Sustain. Energy Rev.*** 112 (2019) 183–194. doi:10.1016/j.rser.2019.05.052.

[48] R. Jadar, K.S. Shashishekar, S.R. Manohara, F-MWCNT Nanomaterial Integrated Automobile Radiator, in: ***Mater. Today Proc., Elsevier Ltd,*** 2017: pp. 11028–11033. doi:10.1016/j.matpr.2017.08.062.

[49] R. Babu Bejjam, K. Nigusie, T. Wondatir, S. Worku, Numerical analysis of water, ethylene glycol and NF based radiator using CFD, ***Mater. Today Proc.*** (2021). doi:10.1016/j.matpr.2021.04.503.

[50] G.K. Batchelor, The effect of Brownian motion on the bulk stress in a suspension of spherical particles, ***J. Fluid Mech***. 83 (1977) 97–117. doi:10.1017/S0022112077001062.

[51] A. Asadi, M. Asadi, M. Rezaei, M. Siahmargoi, F. Asadi, The effect of temperature and solid concentration on dynamic viscosity of MWCNT/MgO (20–80)–SAE50 hybrid nano-lubricant and proposing a new correlation: An experimental study, ***Int. Commun. Heat Mass Transfer***. 78 (2016) 48–53. doi:10.1016/j.icheatmasstransfer.2016.08.021.

[52] X. Han, X. Chen, Q. Wang, S.M. Alelyani, J. Qu, Investigation of CoSO4-based Ag NFs as spectral beam splitters for hybrid PV/T applications, ***Sol. Energy***. 177 (2019) 387–394. doi:10.1016/j.solener.2018.11.037.

[53] A.A.R. Darzi, M. Farhadi, K. Sedighi, R. Shafaghat, K. Zabihi, Experimental investigation of turbulent HT and flow characteristics of SiO 2/water NF within helically corrugated tubes, Int. Commun. ***Heat Mass Transfer***. 39 (2012) 1425–1434. doi:10.1016/j.icheatmasstransfer.2012.07.027.

[54] G. Huminic, A. Huminic, International Journal of Heat and Mass Transfer HT characteristics in double tube helical HXs using NFs, Int. ***J. Heat Mass Transfer***. 54 (2011) 4280–4287. doi:10.1016/j.ijheatmasstransfer.2011.05.017.

[55] H. Bahremand, A. Abbassi, Experimental and numerical investigation of turbulent nano fl uid fl ow in helically coiled tubes under constant wall heat fl ux using Eulerian – Lagrangian approach, ***Powder Technology***. 269 (2015) 93–100. doi:10.1016/j.powtec.2014.08.066.

[56] P.C.M. Kumar, M. Chandrasekar, Heliyon CFD analysis on heat and fl ow characteristics of double helically coiled tube HX handling MWCNT / water nano fl uids, ***Heliyon.*** 5 (2019) e02030. doi:10.1016/j.heliyon.2019.e02030.

[57] R.N. Radkar, B.A. Bhanvase, D.P. Barai, S.H. Sonawane, Intensified convective HT using ZnO NFs in HX with helical coiled geometry at constant wall temperature, ***Mater. Sci. Energy Technology***. 2 (2019) 161–170. doi:10.1016/j.mset.2019.01.007.

[58] K. Singh, S.K. Sharma, S.M. Gupta, An experimental investigation of hydrodynamic and HT characteristics of surfactant-water solution and CNT NF in a helical coil-based HX, ***Mater. Today Proc***. 43 (2020) 3896–3903. doi:10.1016/j.matpr.2020.12.1233.

[59] H. Ravi Kulkarni, C. Dhanasekaran, P. Rathnakumar, S. Sivaganesan, Experimental study on thermal analysis of helical coil HX using Green synthesis silver NF, ***Mater. Today Proc.*** 42 (2020) 1037–1042. doi:10.1016/j.matpr.2020.12.087.

[60] A.F. Niwalkar, J.M. Kshirsagar, K. Kulkarni, Experimental investigation of HT enhancement in shell and helically coiled tube HX using SiO2/ water NFs, Mater. Today Proc. 18 (2019) 947–962. doi:10.1016/j.matpr.2019.06.532.

[61] B.A. Bhanvase, S.D. Sayankar, A. Kapre, P.J. Fule, S.H. Sonawane, Experimental investigation on intensified CHTC of water based PANI NF in vertical helical coiled HX, ***Appl. Therm. Eng.*** 128 (2018) 134–140. doi:10.1016/j.applthermaleng.2017.09.009.

[62] M. Bahiraei, M. Hangi, M. Saeedan, A novel application for energy efficiency improvement using NF in shell and tube HX equipped with helical baffles, *Energy*. 93 (2015) 2229–2240. doi:10.1016/j.energy.2015.10.120.

[63] K. Narrein, H.A. Mohammed, Influence of NFs and rotation on helically coiled tube HX performance, T***hermochim. Acta.*** 564 (2013) 13–23. doi:10.1016/j.tca.2013.04.004.

[64] Milad Zare, Mohammad Mahdi Heyhat, Performance evaluation of nanofluid flow in conical and helical coiled tubes, ***Faculty of Mechanical Engineering, Tarbiat,*** MO dares, University, Tehran, Iran 10 July (2017) doi.org/10.1007/s10973-018-7516-0.3456789().,-volV)(0123456789().,-volV)

[65] M.M. Heyhat, A. Jafarzad, P. Changizi, et al., Experimental research on the performance of nanofluid flow through conically coiled tubes, *Powder Technology* (2019), doi.org/10.1016/j.powtec.2020.05.058.

[66] Fethi M. ALTUNAY, Effect of Nanoparticle Shape and Volumetric Ratio on Nanofluid Flow in Serpentine Micro tubes, K***arabuk University, Department of Mechanical Engineering, Karabuk/Turkey***, Email: fmaltunay@gmail.com

[67] C. Selvam, D. Mohan Lal, S. Harish, Enhanced HT performance of an automobile radiator with graphene based suspensions, ***Appl. Therm. Eng***. 123 (2017) 50–60. doi:10.1016/j.applthermaleng.2017.05.076.

[68] K. Goudarzi, H. Jamali, HT enhancement of Al2O3-EG NF in a car radiator with wire coil inserts, ***Appl. Therm. Eng***. 118 (2017) 510–517. doi:10.1016/j.applthermaleng.2017.03.016.

[69] P. Kumar Rai, A. Kumar, A. Yadav, Experimental Investigation of HT Augmentation in Automobile Radiators using Magnesium Oxide/Distilled Water-Ethylene Glycol based NF, in: ***Mater. Today Proc., Elsevier Ltd.***, 2020: pp. 1525–1532. doi:10.1016/j.matpr.2020.04.472.

[70] X. Li, H. Wang, B. Luo, The thermophysical properties and enhanced HT performance of SiC-MWCNTs hybrid NFs for car radiator system, ***Colloids Surfaces A Physicochem.*** Eng. Asp. 612 (2021) 125968. doi:10.1016/j.colsurfa.2020.125968.

[71] T.J. Choi, S.H. Kim, S.P. Jang, D.J. Yang, Y.M. Byeon, HT enhancement of a radiator with mass-producing NFs (EG/water-based Al2O3 NFs) for cooling a 100 kW high power system, ***Appl. Therm. Eng.*** 180 (2020) 115780. doi:10.1016/j.applthermaleng.2020.115780.

[72] N. Arora, M. Gupta, An updated review on application of NFs in flat tubes radiators for improving cooling performance, ***Renew Sustain Energy Revew.*** 134 (2020) 110242. doi:10.1016/j.rser.2020.110242.

[73] S. Koçak Soylu, İ. Atmaca, M. Asiltürk, A. Doğan, Improving HT performance of an automobile radiator using Cu and Ag doped TiO2 based NFs, ***Appl. Therm. Eng.*** 157 (2019). doi:10.1016/j.applthermaleng.2019.113743.

[74] H. Safikhani, A. Abbassi, A. Khalkhali, M. Kalteh, Multi-objective optimization of NF flow in flat tubes using CFD, Artificial Neural Networks and genetic algorithms, ***Adv. Powder Technol.*** 25 (2014) 1608–1617. doi:10.1016/j.apt.2014.05.014.

[75] H. Safikhani, F. Abbasi, Numerical study of NF flow in flat tubes fitted with multiple twisted tapes, ***Adv. Powder Technol.*** 26 (2015) 1609–1617. doi:10.1016/j.apt.2015.09.002.

[76] S. Ramalingam, R. Dhairiyasamy, M. Govindasamy, Assessment of HT characteristics and system physiognomies using hybrid NFs in an automotive radiator, ***Chem. Eng. Process. - Process Intensif.*** 150 (2020) 107886. doi:10.1016/j.cep.2020.107886.

[77] W. Guo, G. Li, Y. Zheng, C. Dong, Laminar convection HT and flow performance of Al2O3–water NFs in a multichannel-flat aluminum tube, ***Chem. Eng. Res. Des.*** 133 (2018) 255–263. doi:10.1016/j.cherd.2018.03.009.

[78] P. Sharma, V. Kumar, G.S. Sokhal, G. Dasaroju, V.K. Bulasara, Numerical study on performance of flat tube with water based copper oxide NFs, ***Mater. Today Proc.*** 21 (2020) 1800–1808. doi:10.1016/j.matpr.2020.01.234.

[79] A. Alirezaie, M.H. Hajmohammad, A. Alipour, M. salari, Do NFs affect the future of HT?"A benchmark study on the efficiency of NFs," ***Energy***. 157 (2018) 979–989. doi:10.1016/j.energy.2018.05.060.

[80] B. Sun, H. Liu, Flow and HT characteristics of NFs in a liquid-cooled CPU heat radiator, ***Appl. Therm. Eng.*** 115 (2017) 435–443. doi:10.1016/j.applthermaleng.2016.12.108.

[81] G.A. Oliveira, E.M. Cardenas Contreras, E.P. Bandarra Filho, Experimental study on the HT of MWCNT/water NF flowing in a car radiator, ***Appl. Therm. Eng.*** 111 (2017) 1450–1456. doi:10.1016/j.applthermaleng.2016.05.086.

[82] A. Kumar, M.A. Hassan, P. Chand, Heat transport in NF coolant car radiator with louvered fins, ***Powder Technol.*** 376 (2020) 631–642. doi:10.1016/j.powtec.2020.08.047.

[83] N. Zhao, J. Yang, H. Li, Z. Zhang, S. Li, Numerical investigations of laminar HT and flow performance of Al2O3-water NFs in a flat tube, Int. ***J. Heat Mass Transfer.*** 92 (2016) 268–282. doi:10.1016/j.ijheatmasstransfer.2015.08.098.

[84] M.K. Abdolbaqi, R. Mamat, N.A.C. Sidik, W.H. Azmi, P. Selvakumar, Experimental investigation and development of new correlations for HT enhancement and friction factor of BioGlycol/water based TiO2 NFs in flat tubes, Int. ***J. Heat Mass Transfeer***. 108 (2017) 1026–1035. doi:10.1016/j.ijheatmasstransfer.2016.12.024.

[85] S.A. Kaska, R.A. Khalefa, A.M. Hussein, Hybrid NF to enhance HT under turbulent flow in a flat tube, ***Case Stud Therm Eng***. 13 (2019) 4–13. doi:10.1016/j.csite.2019.100398.

[86] A.M. Hussein, H.K. Dawood, R.A. Bakara, K. Kadirgamaa, Numerical study on turbulent forced convective HT using NFs TiO2 in an automotive cooling system, ***Case Stud Therm Eng 9*** (2017) 72–78. doi:10.1016/j.csite.2016.11.005.

[87] J. Zhang, Y. Diao, Y. Zhao, Y. Zhang, Experimental study of TiO2-water NF flow and HT characteristics in a multiport minichannel flat tube, ***Int. J. Heat Mass Transf.*** 79 (2014) 628–638. doi:10.1016/j.ijheatmasstransfer.2014.08.071.

[88] A.M. Elsaid, Experimental study on the HT performance and friction factor characteristics of Co3O4 and Al2O3 based H2O/(CH2OH)2 NFs in a vehicle engine radiator, ***Int. Commun. Heat Mass Transfer.*** 108 (2019) 104263. doi:10.1016/j.icheatmasstransfer.2019.05.009.

[89] R.S. Vajjha, D.K. Das, D.R. Ray, Development of new correlations for the Nu and the friction factor under turbulent flow of NFs in flat tubes, ***Int. J. Heat Mass Transfer.*** 80 (2015) 353–367. doi:10.1016/j.ijheatmasstransfer.2014.09.018.

[90] G. Huminic, A. Huminic, The HT performances and entropy generation analysis of hybrid NFs in a flattened tube, ***Int. J. Heat Mass Transfer***. 119 (2018) 813–827. doi:10.1016/j.ijheatmasstransfer.2017.11.155.

[91] S.A. Ahmed, M. Ozkaymak, A. Sözen, T. Menlik, A. Fahed, Improving car radiator performance by using TiO2-water NF, ***Eng. Sci. Technol. an Int.*** J. 21 (2018) 996–1005. doi:10.1016/j.jestch.2018.07.008.

[92] J. Chen, J. Jia, Experimental study of TiO2 NF coolant for automobile cooling applications, ***Mater. Res. Innov.*** 21 (2017) 177–181. doi:10.1080/14328917.2016.1198549.

[93] P.C.M. Kumar, M. Chandrasekar, Heliyon CFD analysis on heat and fl ow characteristics of double helically coiled tube HX handling MWCNT / water nano fl uids, ***Heliyon.*** 5 (2019) e02030. doi:10.1016/j.heliyon.2019.e02030.

[94] Nanofluid in Heat Exchangers for Mechanical Systems. https://doi.org/10.1016/B978-0-12-821923-2.00001-4 1 Copyright © 2020 Elsevier Inc.

[95] Ho, C., Wei, C., Li, W. An experimental investigation of forced convective cooling performance of a microchannel heat sink with Al_2O_3/water nanofluid, ***Applied Thermal Engineering***, 30 (2-3), 96-103, 2010.

[96] Kalteh, M., Abbassi, A., Avval, M., Frijns, A., Darhuber, D., Harting, J. Experimental and numerical investigation of nanofluid forced convection inside a wide microchannel heat sink, ***Applied Thermal Engineering***, 36 (1), 260-268, 2012.

[97] Aliabadi, M., Rahimpour, F., Sartipzadeh, O., Pazdar, S. Heat transfer enhancement by combination of serpentine curves and nanofluid flow in microtube, ***Experimental Heat Transfer*** 30 (3), 235-252, 2017.

[98] Javaid, M.U.; Cheema, T.A.; Park, C.W. Analysis of Passive Mixing in a Serpentine Microchannel with Sinusoidal Side Walls, ***Micromachines*** , 9(8), 2018.

[99] Uz, K., "Eş eksenli üç borulu ısı değiştiricilerinde nanoakışkan kullanımının sayısal olarak incelenmesi" Yüksek Lisans Tezi, ***Karabük Üniversitesi Fen Bilimleri Enstitüsü***, Karabük, 51-65 (2018).